



**HAL**  
open science

## Formation of halogenated forms of bisphenol A (BPA) in water: Resolving isomers with ion mobility – mass spectrometry and the role of halogenation position in cellular toxicity

Mauricius Marques dos Santos, Caixia Li, Shenglan Jia, Mickaël Thomas, Hervé Gallard, Jean-Philippe Croué, Pascal Carato, Shane Allen Snyder

### ► To cite this version:

Mauricius Marques dos Santos, Caixia Li, Shenglan Jia, Mickaël Thomas, Hervé Gallard, et al.. Formation of halogenated forms of bisphenol A (BPA) in water: Resolving isomers with ion mobility – mass spectrometry and the role of halogenation position in cellular toxicity. *Journal of Hazardous Materials*, 2024, 465, pp.133229. 10.1016/j.jhazmat.2023.133229 . hal-04432106

HAL Id: hal-04432106

<https://univ-poitiers.hal.science/hal-04432106v1>

Submitted on 20 Nov 2024

**HAL** is a multi-disciplinary open access archive for the deposit and dissemination of scientific research documents, whether they are published or not. The documents may come from teaching and research institutions in France or abroad, or from public or private research centers.

L'archive ouverte pluridisciplinaire **HAL**, est destinée au dépôt et à la diffusion de documents scientifiques de niveau recherche, publiés ou non, émanant des établissements d'enseignement et de recherche français ou étrangers, des laboratoires publics ou privés.



Distributed under a Creative Commons Attribution - NonCommercial - NoDerivatives 4.0 International License



## Research Paper

# Formation of halogenated forms of bisphenol A (BPA) in water: Resolving isomers with ion mobility – mass spectrometry and the role of halogenation position in cellular toxicity

Mauricius Marques dos Santos<sup>a</sup>, Caixia Li<sup>a</sup>, Shenglan Jia<sup>a</sup>, Mikael Thomas<sup>b</sup>, Hervé Gallard<sup>b</sup>, Jean-Philippe Croué<sup>b</sup>, Pascal Carato<sup>c,d</sup>, Shane Allen Snyder<sup>a,\*</sup>

<sup>a</sup> Nanyang Environment & Water Research Institute (NEWRI), Nanyang Technological University, CleanTech One, 1 Cleantech Loop, 637141, Singapore

<sup>b</sup> Institut de Chimie des Milieux et des Matériaux de Poitiers, IC2MP UMR 7285 CNRS, Université de Poitiers, France

<sup>c</sup> Laboratoire Ecologie & Biologie des Interactions, UMR CNRS 7267, Université de Poitiers, France

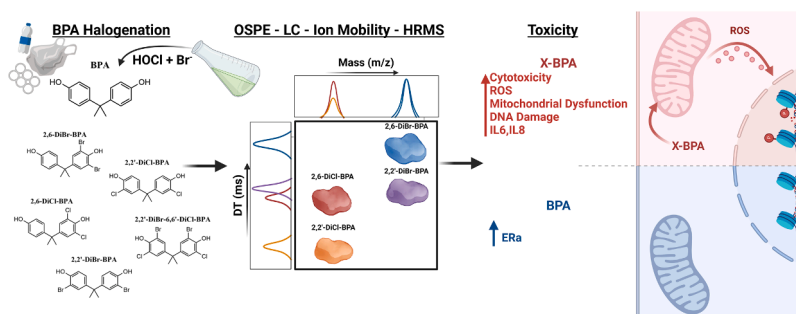
<sup>d</sup> INSERM CIC1402, Université de Poitiers, IHES Research Group, Poitiers, France



## HIGHLIGHTS

- OSPE-LC-IM-HRMS enables analysis of multiple isomeric XBPA species.
- XBPA shows greater impacts on cell cytotoxicity and cell bioenergetics than BPA.
- Presence of halogen atoms in positions 2 or 2' is correlated with increased toxic effects.
- DNA damage was observed for BPA chlorinated water samples.

## GRAPHICAL ABSTRACT



## ARTICLE INFO

Editor: Karina S. B. Miglioranza

## Keywords:

Bisphenol A  
Ion-mobility-high-resolution-mass-spectrometry (IM-HRMS)  
Chlorination  
Disinfection by-products (DBPs)  
Toxicity

## ABSTRACT

Halogenated BPA (XBPA) forms resulting from water chlorination can lead to increased toxicity and different biological effects. While previous studies have reported the occurrence of different XBPA, analytical limitation have hindered the analysis and differentiation of the many potential isomeric forms. Using online solid-phase extraction - liquid chromatography - ion-mobility - high-resolution mass spectrometry (OSPE-LC-IM-HRMS), we demonstrated a rapid analysis method for the analysis of XBPA forms after water chlorination, with a total analysis time of less than 10 min including extraction and concentration and low detection limits (~5–80 ng/L range). A multi in-vitro bioassay testing approach for the identified products revealed that cytotoxicity and bioenergetics impacts were largely associated with the presence of halogen atoms at positions 2 or 2' and the overall number of halogens incorporated into the BPA molecule. Different XBPA also showed distinct impacts on oxidative stress, peroxisome proliferator-activated receptor gamma - PPAR $\gamma$ , and inflammatory response. While increased DNA damage was observed for chlorinated water samples ( $4.14 \pm 1.21$ -fold change), the additive effect of the selected 20 XBPA studied could not explain the increased DNA damage observed, indicating that additional species or synergistic effects might be at play.

\* Corresponding author.

E-mail address: [ssnyder@ntu.edu.sg](mailto:ssnyder@ntu.edu.sg) (S.A. Snyder).

<https://doi.org/10.1016/j.jhazmat.2023.133229>

Received 28 September 2022; Received in revised form 5 December 2023; Accepted 9 December 2023

Available online 13 December 2023

0304-3894/© 2023 The Authors. Published by Elsevier B.V. This is an open access article under the CC BY-NC-ND license (<http://creativecommons.org/licenses/by-nc-nd/4.0/>).

## 1. Introduction

Bisphenol A (BPA) is a chemical additive used in the manufacturing of many plastics and resins and found in a plethora of consumer products. Despite having its use regulated and restricted in many countries [1], BPA is still used in many applications, with an estimated production of 7 million tons [2,3]. Given its widespread usage, BPA has been reported to occur in the most diverse set of environments, being detected in many organisms, including humans [4,5].

BPA occurrence in source water can vary from ng/L to µg/L concentrations [6], importantly its leaching from water bottles can also lead to exposures in the µg/L range [7]. In a recent study of drinking water samples in France, BPA was detected in 29% of all samples in concentration up to 229 ng/L, with this same study reporting the occurrence of halogenated BPA forms in 51% of samples [8]. Sensitive populations, such as infants are also particularly susceptible due to leaching from plastic bottles [9].

BPA is an endocrine disrupting chemical (EDC), and some reports suggest adverse consequences derived from exposure to BPA even at a low concentration [10,11]. Although many alternatives or analogues are already available, they also pose several health concerns [12,13]. Notably, tetrabromo-BPA (TBPA) and tetrachloro-BPA (TCBPA) have current commercial application as flame retardants and have been linked to different effects affecting the endocrine system leading to dysregulation of lipid metabolism as obesogens and activation of estrogen receptors (ER $\alpha$  and ER $\beta$ ) [14,15].

Upon introduction to the environment, BPA is subject to many transformations and given its use in many consumer products, the formation of halogenated-BPA (XBPA) forms is of concern [16]. The formation of XBPA can occur when BPA present in tap water or leaching from other materials in contact with water (i.e., water bottles) reacts with chlorine based oxidants added to tap water as disinfectants [17]. A recent review of studies published from 2002 to 2021 highlights that chlorinated forms of BPA have been reported as endocrine disruptors, and are associated with obesity, type II diabetes and myocardial infarction [16]. Indeed, previous work has reported the formation of XBPA in different systems [17–19], with tap water considered as the first route of exposure for humans [8,16,18]. XBPA have also been detected in many biological matrices such as urine, breast milk, serum and placental tissue [20–23]. While chlorinated species can be expected in the presence of chlorine-based disinfectants in water, other halogens such as bromine and iodine can also be formed [2]. The presence of low concentrations of bromide in source waters is a commonly observed feature and its concentration can be exacerbated in coastal regions due to salt water intrusion [24].

However, while previous studies have shown the formation of a diverse set of XBPA after chlorination with or without the presence of halide ions, such works usually did not focus on identifying or distinguishing different isomers formed, nor on potential differences in their toxicity and associated health impacts [2,25]. Even many studies focusing on the human exposure of biological samples lack information regarding potential isomers [26,27]. Much of this information gap is caused by current instrument limitations. Mainly the fact that the widely used mass-spectrometry approaches, and in specific (ultra) high-resolution mass spectrometry (HRMS) cannot distinguish substitution positions [28].

While the combination of ion-mobility spectrometry, the gas-phase separation of ions based on size and shape, with mass spectrometry has been proposed since the early 1960's [29], only since the early 2000's with the introduction of the first commercial ion-mobility-mass spectrometers (IM-MS) systems its use has gained traction [30]. However, most applications are still focused on the different areas related to the analysis of biological molecules [31–34]. Only in recent years, the use of IM-HRMS has found some applications for environmental contaminants and/or hazardous materials, most notably per- and poly-fluoroalkyl substances (PFAS) [35–38]. Another study comparing 56

small molecules of environmental relevance (Contaminants of Emerging Concern) using different commercial IM instrument types further highlights the potential of such techniques [39]. A recent review on emerging technologies to enable rapid chemical characterization of mixtures has highlighted the potential, and need, for a combination of high-throughput solid-phase extraction systems and IM-MS techniques for non-targeted screening (NTA) assessments [40], however, few works have explored the coupling of solid-phase extract (SPE)-IM-HRMS [41].

While many studies of novel disinfection byproducts focus on cytotoxic effects [42], the study of more subtle effects is necessary to better understand the mechanisms of toxicity and to provide earlier signs of potential deleterious effects. Dysfunction of cellular bioenergetics processes and oxidative stress an example of processes that have been previously investigated to assess the effects of environmental samples and novel chemicals and transformation products to human cells [43–45]. Inflammatory responses are another effects that could lead to serious effect that are many times overlooked, and the study of different biomarkers such as Interleukin-6 (IL6) and Interleukin-8 (IL8), have been shown to be early and sensitive signals [44,46].

In this work we seek to understand the formation and toxicity of different halogenated forms of BPA under different water chlorination conditions in the presence of bromide ions. We applied a comprehensive approach to understand the basis of increased toxicity upon chlorination of waters containing BPA. Using a set of analytical tools tailored to overcome many of previous studies limitations regarding the different isomeric forms of XBPA, we introduced the use of OSPE-LC-IM-HRMS analysis enabling quick sample preparation, concentration and analysis in 10 min, while also addressing the critical challenge of monitoring the formation of different structural isomers upon chlorination or bromination of the BPA rings. We also evaluated the potential roles of halogenation position on BPA rings and its impact on cellular toxicity using a multi-biomarker approach [47,48] with different endpoints for cell cytotoxicity, cellular bioenergetics, oxidative stress, ER $\alpha$  and PPAR $\gamma$  activation and inflammatory response with IL6 and IL8 cytokines.

## 2. Materials and methods

### 2.1. Chemical and reagents

All chemicals and materials were obtained from commercial sources and used without further purification unless otherwise stated. Bisphenol A (BPA), dimethyl sulfoxide (DMSO), potassium bromide, sodium hypochlorite solution (4–5% active chlorine) and sodium thiosulfate 99% were purchased from Sigma-Aldrich. LC-MS grade (Optima LC/MS) solvents and reagents (water, acetonitrile, methanol, 2-propanol, and formic acid) were purchased from Fisher Scientific. Ultrapure water (18.2 M $\Omega$ -cm) was produced by a Milli-Q EQ 7000 water purification system (Millipore). HepG2 (HB-8065) cells were purchased from American Type Culture Collection (ATCC). Dulbecco's Modified Eagle Medium (DMEM), Dulbecco's phosphate-buffered saline (DPBS), certified foetal bovine serum (FBS), trypan blue solution (0.4%), alamarBlue HS cell viability assay, HCS DNA damage kit, high-capacity cDNA reverse transcription kit, RNaseOUT (40 U/µL), NucBlue Live ReadyProbes Reagent and RNase Cocktail Enzyme Mix were purchased from Thermo Fisher Scientific. Maxwell® RSC simplyRNA Tissue Kit was purchased from Promega Corporation. Gene expression assay primer and probes and PrimeTime Gene Expression Master Mix were purchased from Integrated DNA Technologies (IDT). Seahorse XF Cell Mito Stress Test Kit, Seahorse XFe96 FluxPak, Seahorse XF DMEM assay medium, 1.0 M Glucose Solution, 100 mM Pyruvate Solution, 200 mM Glutamine Solution and RTCA E-plates PET microwell plates were purchased from Agilent Technologies. Halogenated BPA standards were synthesized chemically and purified by group's organic chemistry laboratory (IHES research group, EBI/CIC INSERM 1402), and its purity was assessed to be > 97%. Details of product synthesis were described previously [18].

## 2.2. OSPE chlorination experiments

BPA chlorination experiments were done in 6 mL glass vials (suitable for OSPE-LC analysis) with PTFE/Silicone septa. Five mL of a 5 mM phosphate buffer solution (pH  $7.0 \pm 0.1$ ) spiked with 10  $\mu\text{M}$  of BPA were treated for 60 min with different free chlorine concentrations (5  $\mu\text{M}$ , 10  $\mu\text{M}$ , 20  $\mu\text{M}$ , 40  $\mu\text{M}$  and 80  $\mu\text{M}$ ) and for each free-chlorine condition bromide ions concentration was also varied (0  $\mu\text{M}$ , 5  $\mu\text{M}$ , 10  $\mu\text{M}$ , 20  $\mu\text{M}$  and 60  $\mu\text{M}$ ). Free-chlorine and bromide ions concentration ranges were selected to represent a range commonly found during drinking water disinfection steps and at water distribution systems [45,49]. While selected BPA concentration was higher than those observed in drinking water [8,50], it was representative of the concentrations observed from leaching studies of plastic water bottles [51]. Working solutions of free chlorine and bromide ion from sodium hypochlorite and potassium bromide, respectively, were prepared freshly before each experiment batch. Residual chlorine was measured by the N, N-diethyl-p-phenylenediamine (DPD) method (Hach D900 Portable Colorimeter) [52]. At the end of each experiment residual free chlorine was quenched with slight molar excess of sodium thiosulfate 2 M solution (25% excess), although no ideal universal quencher has been reported [53], the use of such quenching agent for analysis of phenolic DBPs has been shown to be suitable [54]. Experiments were done in triplicate ( $n = 3$ ). Samples were stored at 4 °C in the OSPE multisampler and immediately queued for analysis. Free chlorine concentrations used are within ranges to be expected in different conditions in water treatment plants and water distribution networks [45,49]. Bromide concentration range was also within that of WHO drinking water guidelines of less than 6 mg/L.

## 2.3. OSPE-LC-IM-HRMS and data processing

Online solid-phase extraction system consisted of a 1260 Infinity II quaternary pump for SPE conditioning, loading and equilibration; a 1260 Infinity II multisampler with a 900  $\mu\text{L}$  metering head and multi-draw capability for large volume injection; a 1290 Infinity flexible cube with a set of two 2 positions/10 ports valves for liquid flow management; and a 1290 Infinity II multicolumn thermostat with a 6 positions/14 ports valve for multi-SPE cartridge selection. All modules and accessories for the OSPE system were from Agilent Technologies. A detailed description and diagram for this system is presented on Figure S1. LC separation after OSPE was done using a 1290 Infinity II LC system made of a binary pump and multicolumn thermostat with a 2 positions/6 ports valve. Drift-tube ion mobility/QTOF analysis was done using an Agilent Technologies 6560B HRMS system. Detailed OSPE, LC and IM/HRMS parameters are presented on Table S1.

IM-HRMS data was firstly treated using Pacific Northwest National Laboratory (PNNL) Preprocessor (Version 4.0) for data interpolation, demultiplexing, multidimensional smoothing, thresholding (250 counts), spike removal and saturation repair [55]. Mass calibration and single-field collision cross section (CCS) calibration was done using Agilent's IM-MS Reprocessor (Version 10.0) and IM-MS Browser (Version 10.0). IM-HRMS features were processed using Agilent's Mass Profiler (Version 10.0), features are unidentified compounds represented by retention time, mass and CCS value. Features were exported as.CEF files and processed using Agilent's high resolution demultiplexing (HRdm 2.0) software. Demultiplexed files were once again processed using Mass Profiler and final.CEF files were used for differential statistical analysis using Agilent's Mass Profiler Professional (MPP) (Version 15.0).

## 2.4. Large volume chlorination experiments and sample preparation

For other assays apart from OSPE-LC-IM-HRMS analysis and NPOC/POC testing, 2 L samples of 5 mM phosphate buffer solution (pH 7.0) spiked with 10  $\mu\text{M}$  of BPA were treated for 60 min with different free

chlorine concentrations (20  $\mu\text{M}$ , 40  $\mu\text{M}$  and 80  $\mu\text{M}$ ) and for each free-chlorine condition bromide ions concentration was also varied (0  $\mu\text{M}$ , 10  $\mu\text{M}$ , and 60  $\mu\text{M}$ ). Conditions were chosen to represent the diverse set of halogenated BPA forms observed during OSPE-LC-IM-HRMS analysis. Residual chlorine was measured by DPD method (Hach D900 Portable Colorimeter). At the end of each experiment residual free chlorine was quenched with slight molar excess of sodium thiosulfate 2 M solution (25% excess). Experiments were done in triplicate ( $n = 3$ ). Samples were immediately extracted using an automated SPE system (Autotrace, Dionex/Thermo Fisher Scientific) using 500 mg/ 6 mL HLB cartridges and method previously described by our team [56]. For toxicity and other bioassays extracts were concentrated and solvent exchanged to DMSO using a vacuum concentrator system (SpeedVac, SPD300DDA, Thermo Fisher Scientific). Final extract had a concentration factor of 10, 000x. For extractable organic halogens initial SPE extracts (200x) were further diluted in methanol to a 40x concentration factor.

## 2.5. Extractable organic halogens

Extractable organic chlorine and bromine content was determined using a combustion ion chromatography (CIC) system. System consisted of a fully automated liquid autosampler (MMS 5000, Analytik Jena), an absorber module (920 Absorber Module, Metrohm) and an IC system with a conductivity detector (940 Professional IC Vario, Metrohm). For analysis, 30  $\mu\text{L}$  of a 40x concentrated SPE extract in methanol were injected into the combustion module. System control and data processing was done using MagIC Net (Version 4.0) software. Detailed method parameters are presented on Table S2.

## 2.6. Non-purgeable organic carbon (NPOC)/Purgeable organic carbon (POC)

NPOC/POC analysis was done using a TOC-LCH system with ASI-L autosampler (Shimadzu). Chlorination experiments were done as described previously for OSPE-LC-IM-HRMS analysis; however, BPA, free chlorine and bromide ions concentrations were all increased by a factor of 10x due to instrument sensitivity and experiments were conducted in 24 mL precleaned TOC vials with no headspace left after quenching. Sparging time was set as 5 min

## 2.7. Cell culture

HepG2 cells were maintained in DMEM culture media supplemented with 10% FBS at 37 °C and 5% CO<sub>2</sub> atmosphere, media was exchanged twice a week and cells were subcultured before reaching confluence (80–90%). Cells were counted by trypan blue exclusion using an automated cell-counter (Countess II FL, Thermo Fisher Scientific).

## 2.8. Cytotoxicity

Cell viability measurements were done using AlamarBlue HS reagent. Briefly, 5000 HepG2 cells in 40  $\mu\text{L}$  of 2% FBS phenol red free DMEM media were seeded into 384 well microplates using a MultiFlo FX multimode dispenser (BioTek, Agilent Technologies). Plates were incubated for 18 h at 37 °C in a 5% CO<sub>2</sub> atmosphere. Test extracts or chemicals were dosed into well using a digital dispenser (Multidrop Pico 8, Thermo Fisher Scientific) with D8+ cassettes, DMSO concentration was normalized to 0.5% automatically with large volume D4+ dispensing cassettes. Dose-response curves were created using  $\frac{1}{4}$  log dilution from maximum concentration achievable (0.5% DMSO) from 100 mM stock solutions or 10,000x extracts, 12-point curves were created with six replicates for each concentration. After extract addition plates were incubated for 24 h, 48 h or 72 h as indicated in each experiment at 37 °C in a 5% CO<sub>2</sub> atmosphere. After incubation, 4  $\mu\text{L}$  of AlamarBlue HS reagent was added to each well using the MultiFlo FX multimode dispenser. Plates were again incubated for 2 h in the same

environmental conditions described before and then fluorescent signal intensity was measured using a multimode microplate reader (Cytation 5, BioTek, Agilent Technologies).

### 2.9. Real-time cell analysis (impedance)

Real-time cell analysis impedance measurements were done accordingly to recently described protocols using a xCELLigence RTCA eSight system (Agilent Technologies) with minor modifications [52]. Briefly, 20,000 HepG2 cells in 100  $\mu$ L of DMEM phenol-red free media supplemented with 2% FBS were seeded in each well of a 96-well (E-plate 96 PET) overnight for 18 h. After incubation, test compounds were added at described concentrations in each experiment ( $n = 6$ ) for a total well volume of 150  $\mu$ L. Impedance measurements were recorded every 15 min for 400 cycles (~4 days). Results are presented as % of control (DMSO at 0.1%). Experiments were conducted at 37 °C and 5% CO<sub>2</sub> atmosphere.

### 2.10. ER $\alpha$ agonist assay

ER $\alpha$  response was monitored using a gene reporter cell line (GeneBLazer ER $\alpha$ -UAS-bla GriPTite Cells). Cell culture and assay was done accordingly to manufacturer user guide using non-division arrested cells. Briefly, in 384-well microplates, 20,000 cells in 32  $\mu$ L of assay medium were incubated for 24 h at 37 °C in a 5% CO<sub>2</sub> atmosphere. Cells were then treated with extracts or chemicals for 16 h at 37 °C in a 5% CO<sub>2</sub> atmosphere. Curves for BPA halogenated forms were generated using the same digital dispenser procedure described for cytotoxicity section ( $n = 5$  for each concentration level). After incubation, 8  $\mu$ L of substrate mix containing FRET B/G (CCF4-AM) reagent were added to each well and plates were incubated for 2 h at room temperature in the dark. Fluorescent signal in the blue channel and FRET signal in the green channel were measured according to cell line protocol using a multimode microplate reader (Cytation 5, BioTek, Agilent Technologies). Cell-free control wells were used for background subtraction. Blue/green emission ratios for each well were calculated by dividing the background-subtracted blue emission values by the background-subtracted green emission values. Reference dose-response curves for 17- $\beta$ -estradiol and BPA were used for further data analysis. A representative dose-response curves for both controls are presented in Figure S2.

### 2.11. Mitochondrial stress test (MST)

Cell bioenergetics experiments were done using an extracellular flux analyser (Seahorse XFe 96, Agilent Technologies) according to manufacturer instructions as previously described for acute exposure experiments [44]. Briefly, 20,000 HepG2 cells were seeded into extracellular flux assay plates with 100  $\mu$ L of culture medium. Cells were incubated in a 5% CO<sub>2</sub> incubator for 18 h at 37 °C in a 5% CO<sub>2</sub> atmosphere. After media exchange to DMEM extracellular flux media and equilibration, exposure to test substances was achieved through an injection from one of the ports of the system cartridge. Electron transport chain modulators: oligomycin, FCCP, and rotenone/antimycin A were added to obtain final concentrations of 1  $\mu$ M, 1  $\mu$ M, and 0.5  $\mu$ M, respectively through the remaining ports of the system cartridge. Values of each measurement were given as oxygen consumption rate (OCR, pmol O<sub>2</sub>/min/10,000 cells). Cell number was used to normalize OCR data via a standard DAPI assay (NucBlue Live Ready Probes Reagent, Thermo Fisher Scientific).

### 2.12. Real-time oxidative stress

Real-time oxidative stress assay was done using CellROX green fluorescent dye for ROS monitoring and NucBlue Live reagent for cell number monitoring (Thermo Fisher Scientific). 20,000 HepG2 cells in 100  $\mu$ L of DMEM phenol-red free media supplemented with 2% FBS were

seeded in each well of a 96-well thin-plastic bottom microplate. Cells were incubated for 18 h at 37 °C in a 5% CO<sub>2</sub> atmosphere. After incubation, test compounds at described concentrations were added to cells together 11  $\mu$ L of a 50  $\mu$ M solution of CellROX green dye diluted in NucBlue Live reagent. Cell images were acquired using a xCELLigence RTCA eSight system (Agilent Technologies). Two images per well were acquired using a 10x magnification lens in both brightfield, and, blue and green fluorescent channels. Acquisition time for fluorescent channels was set at 200 ms and images were acquired every 20 min for 16 h. Images were processed using RTCA eSight Software and are presented as fold-change over DMSO control.

### 2.13. DNA damage

DNA damage was assessed using the double-strand break (DSB) marker phosphorylated H2AX (Ser139). Assay was done accordingly to manufacturer instructions (HCS DNA Damage Kit, Thermo Fisher Scientific) and previously published protocols [45,52]. Briefly, 20,000 HepG2 cells in 100  $\mu$ L of DMEM phenol-red free media supplemented with 2% FBS were seeded in each well of a 96-well microplate and incubated for 18 h at 37 °C and 5% CO<sub>2</sub> atmosphere. Test compounds were added at described concentrations in each experiment and incubated for 48 h. After incubation, cells were rinsed, fixed permeabilized and stained according to manufacturer instructions. Images were acquired on a CellInsight CX7 LZR high-content analyser (HCA) platform (Thermo Fisher Scientific). Images were acquired at 10x magnification, with 9 fields acquired per microplate well. Results are presented as fold-change in nuclear intensity of pH2AX over control samples (DMSO 0.1%).

### 2.14. Gene expression (qPCR)

Relative gene expression experiments were done using probe-based quantitative polymerase chain reaction (qPCR) assays (Integrated DNA Technologies, IDT), a list of assays used is presented on Table S3. 200,000 HepG2 cells were seeded into 6-well plates in 2 mL of DMEM phenol-red free media supplemented with 2% FBS and incubated for 18 h at 37 °C in a 5% CO<sub>2</sub> atmosphere. After initial incubation, cells were then treated with test compounds at 10  $\mu$ M concentration and incubated for 24 h at 37 °C in a 5% CO<sub>2</sub> atmosphere. After incubation, assay media was removed, and cells were rinsed once with warm DPBS. RNA extraction and purification was done using a Maxwell RSC SimpleRNA Cells Kit protocol (Promega Corporation) following manufacturer instructions. Processing after cell pellet homogenization and lysis was done using an automated nucleic acid extraction system (Maxwell RSC 48, Promega Corporation). cDNA synthesis was done in 20  $\mu$ L reactions using the high-capacity cDNA reverse transcription kit (Thermo Fisher Scientific). 5  $\mu$ L qPCR reactions were assembled in 384-well plates with 2.5  $\mu$ L of PCR master mix, 0.25  $\mu$ L of a 20  $\times$  assay mix (forward and reverse primers, probes) and 0.25  $\mu$ L of a 20  $\times$  housekeeping gene assay mix, and 2  $\mu$ L of cDNA template. Assays mixes were loaded into the plates using a digital dispenser (Multidrop Pico 8, Thermo Fisher Scientific) with D8+ cassettes. PCR cycling protocol followed manufacturer instructions for a fast-cycling program for a total of 40 cycles. Analysis was done using a QuantStudio 7 Pro Real-Time PCR system (Thermo Fisher Scientific) and Design and Analysis Software (Version 2.6). Samples were normalized using delta-delta Ct method with a housekeeping gene (PPIA). Results are presented as fold-change over control samples. Nucleic acid quality and quantity was evaluated using a microvolume UV-Vis spectrophotometer (NanoDrop OneC, Thermo Fisher Scientific).

### 2.15. Statistical analysis

All data are expressed as the mean  $\pm$  SEM/SD, with  $n = 3 - 6$ . EC<sub>50</sub> values were determined using an asymmetric sigmoidal, 5PL model with

log transformed concentrations. Statistical analysis was performed using GraphPad Prism version 9.4.1 for Windows, GraphPad Software, San Diego, California USA. To evaluate differences between treatments and groups one-way analysis of variance (ANOVA) with a Dunnett's multiple comparison post hoc test was used.

### 3. Results and discussion

#### 3.1. Formation of halogenated BPA from water chlorination in the presence of bromide ions

Previous works have demonstrated that chlorine reacts rapidly with phenol-type contaminants such as BPA to form halogenated analogues [2,57]. At the lowest Cl<sub>2</sub>:BPA ratio used (0.5) and without bromide ions

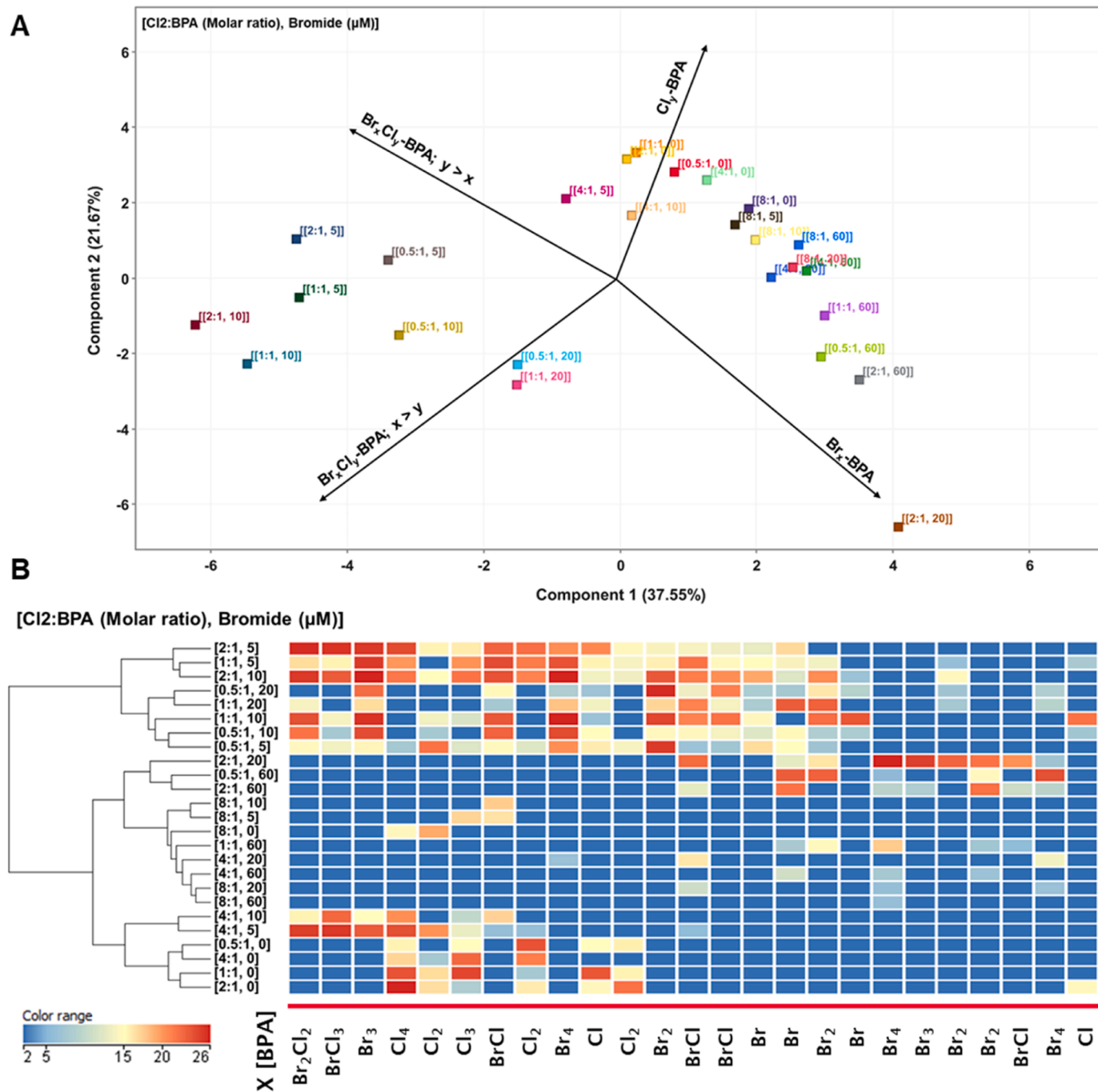


Fig. 1. Formation XBPA forms from water chlorination in the presence of bromide ions. Results of differential statistical analysis from OSPE-LC-IM-HRMS analysis A) Principal component analysis (PCA) of identified features, sample variables are Cl<sub>2</sub>:BPA ratio and Br<sup>-</sup> concentration. B) Hierarchical clustering analysis (HCA), colour range represents average log<sub>2</sub> transformed ion volumes (n = 3).

or in low bromide concentrations (5 and 10  $\mu\text{M}$ ), BPA reduction of 57%, 54%, and 53% was roughly similar to the  $\text{Cl}_2$ :BPA ratio of 0.5, Figure S3A. Presence of high concentrations of bromide ions (60  $\mu\text{M}$ ) significantly reduced the degradation efficiency of BPA upon chlorination, especially at lower chlorine ratios (0.5, 1.0, and 2.0), Figure S3B. At higher ratios (i.e., 4.0 and 8.0) most BPA in solution was transformed due to the presence of high residual oxidant concentrations ( $10.2 \pm 1.2 \mu\text{M}$  and  $26.9 \pm 3.5 \mu\text{M}$ , respectively).

At lower chlorine ratios, untargeted analysis reveals the formation of mostly a diverse set of mono-halogenated species, Fig. 1A. Formation of  $\text{Cl}_x$ -BPA species is favoured only in the absence of bromide ions or, at a lower extent, at high chlorine ratios and low bromide ion concentrations. The relative abundance of  $\text{Br}_x\text{Cl}_y$ -BPA forms identified are presented on Figure S4. Not unexpectedly, formation of  $\text{Br}_y$ -BPA forms is

not usually favoured, being observed mostly at 2:1  $\text{Cl}_2$ :BPA ratios and in the presence of 20 or 60  $\mu\text{M}$  bromide. Formation of mixed  $\text{Br}_x\text{Cl}_y$ -BPA forms was mostly observed at lower ratios  $\text{Cl}_2$ :BPA (0.5 and 1) and lower  $\text{Br}^-$  concentrations (5 and 10  $\mu\text{M}$ ). At such conditions the greatest diversity of XBPA forms was observed (Fig. 1B). At higher  $\text{Cl}_2$ :BPA ratios (4 or 8), opening of aromatic rings of BPA might occur, as described by previous studies leading to the lowest diversity of compounds formed [17].

The preferred formation of brominated species over chlorinated ones might be explained by the greater apparent rate constant of bromine with BPA ( $4.10 \times 10^5 \text{ M}^{-1}\text{s}^{-1}$ ) [58] versus the rate constant reported for the reaction with chlorine ( $62 \text{ M}^{-1}\text{s}^{-1}$ ) [57], both at pH 7. While no rate constant for the reaction with  $\text{Br}_x\text{BPAs}$  is available, the rate constants for reactions between bromine and halophenols have been previously

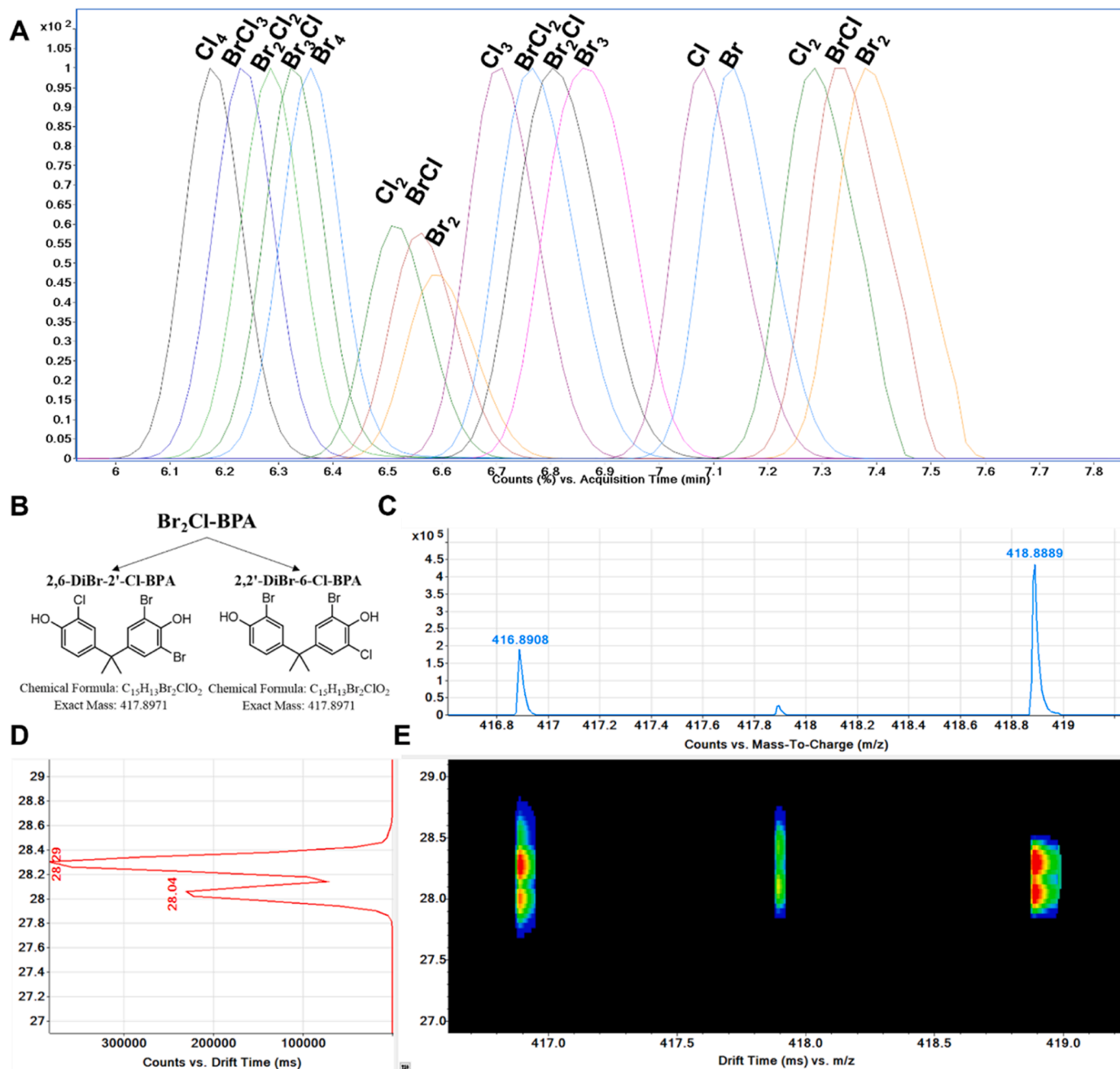


Fig. 2. Analysis of different XBPA isomers. A) Extracted Ion Chromatogram (EIC) for the rapid LC separation of 20 different XBPA species. B) Structures of two potential  $\text{Br}_2$ -Cl-BPA forms. C) Mass spectrum for  $\text{Br}_2$ -Cl-BPA peak. D) Mobiligram for  $\text{Br}_2$ -Cl-BPA LC peak. E) Combined drift-time vs.  $m/z$  plot illustrating separation of isomeric forms of  $\text{Br}_2$ -Cl-BPA.

reported (the rate constants for HOBr with halophenols are also in the same order of  $10^5 \text{ M}^{-1}\text{s}^{-1}$  at pH 7). The reactivity of brominated phenols is also higher than that of unsubstituted phenol at pH 7 due to the lower pKa of brominated phenols, leading to higher concentrations of deprotonated reactive forms [59]. Thus, in the presence of bromide with slight excess of BPA, bromine is rapidly formed and consumed by not only BPA but also by  $\text{Br}_x\text{BPA}$  forms. Thus, less oxidant is available for transformation of BPA resulting in the lower degradation observed in the presence of  $60 \mu\text{M Br}^-$ . The concern for the formation of XBPA species is also highlighted by reports of their occurrence in different water samples [13,18] and also in human samples [26,27]. Given the rapid reaction kinetics of phenols with chlorine the reaction time selected was deemed sufficient for complete reaction of BPA with added chlorine [57]. We do however recognize that the study of multiple time point could have provided additional information of interest. We also recognize that the BPA concentration is generally higher than that observed in environmental samples, however our focus was in studying realistic free chlorine to BPA ratios. We also note that the used concentration used was still in the parts per million range ( $\sim 2.3 \text{ mg/L}$ ).

### 3.2. Structural isomers separation and XBPA identification

Untargeted differential analysis using OSPE-LC-IM-HRMS data shows the formation of multiple species with the same exact mass. Using selected group of 20 structures among potential and observed XBPA structures with chemically synthesized standards, we demonstrated the separation of a complex mixture of XBPA, Fig. 2. While the rapid chromatography was able to achieve some separation of different XBPA forms, especially for dihalogenated forms ( $\text{Br}_2\text{-BPA}$ ,  $\text{BrCl-BPA}$ , and  $\text{Cl}_2\text{-BPA}$ ), Fig. 2A, this method was not good enough to unequivocally identify each component because most components are coeluting and no baseline separation was achieved. However, with the use of HRMS the confidence in the identification can be further improved. This still leaves doubts about several unresolved isomeric pairs. As an example, two  $\text{Br}_2\text{-Cl-BPA}$  forms (2,6-DiBr-2'-Cl-BPA and 2,2'-DiBr-6-Cl-BPA) are presented on Fig. 2B. For such structures, given their same exact mass, no differentiation can be achieved at any mass-resolution, with both structures resulting in the same mass spectrum, Fig. 2C. The two isomers, however, have different drift-time values and can be separated by their CCS values (Fig. 2D). Combining all three dimensions of separation (RT,  $m/z$  and drift-time) a separation of species was possible (Fig. 2E). In total we have established the separation of 6 isomeric pairs, out of which

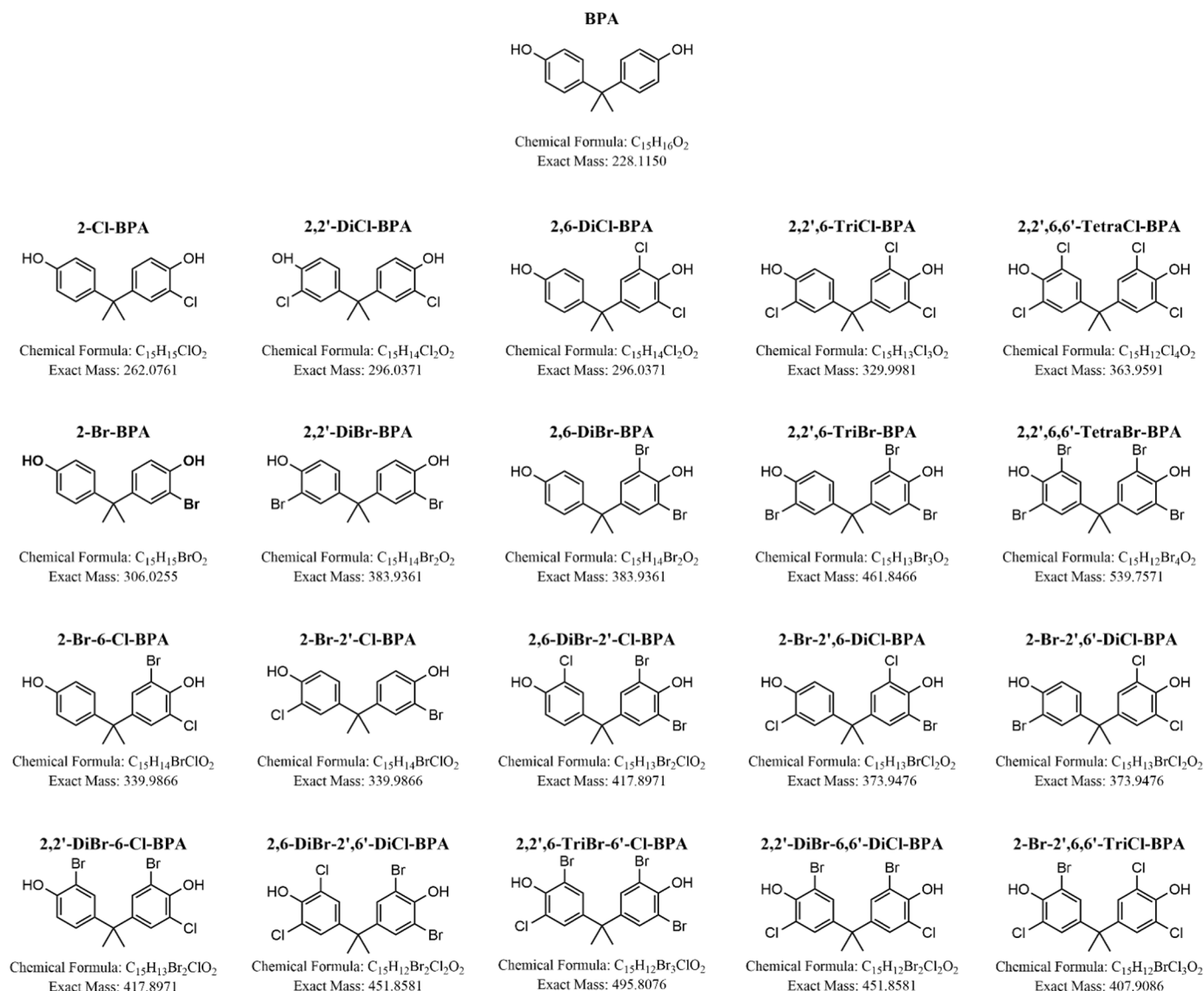


Fig. 3. Structures, molecular formula and accurate mass for BPA and halogenated BPA forms used for further toxicity testing.

3 were resolved in two dimensions (RT and CCS) (DiBr-BPAs - 2,6-DiBr-BPA and 2,2'-DiBr-BPA, Br-Cl-BPAs - 2-Br-6-Cl-BPA and 2-Br-2'-Cl-BPA, and, DiCl-BPAs - 2,6-DiCl-BPA and 2,2'-DiCl-BPA), and three others were resolved by their CCS (Br-DiCl-BPAs - 2-Br-2',6-DiCl-BPA and 2-Br-2',6'-DiCl-BPA, DiBr-DiCl-BPAs - 2,2'-DiBr-6,6'-DiCl-BPA and 2,6-DiBr-2',6'-DiCl-BPA, and, DiBr-Cl-BPAs - 2,2'-DiBr-6-Cl-BPA and 2,6-DiBr-2'-Cl-BPA), Figure S5. Table S4 presents results for the separation of all 20 structures using the developed method, and Fig. 3 shows the structures of each molecule. Selected 20 XBPA molecules corresponded to 46 to 81% of the total ion chromatogram (TIC) intensity, depending on the different experimental conditions.

### 3.3. Toxicity of water extracts

The incorporation of halogen atoms into aromatic organic compounds has been linked to increased toxicity, with the majority of the total organic halogen content in drinking water remaining unknown [60]. Analysis of extractable organic halogen (EOX) fractions revealed that after water chlorination formation of extractable organic chlorine (EOCl) and extractable organic bromine (EOBr) compounds was dependent on chlorine dose, with a decreasing halogen content at higher

doses (Fig. 4A). Increasing bromide concentration also tends to favour the formation of mostly brominated compounds. The decreased incorporation rates shown by EOX analysis might reflect an increased formation of volatile/or purgeable organic fraction, Fig. 4B. Similar to total organic carbon (TOC) measurements, extractable organic halogens in our study refers to any organic species containing Cl or Br atoms. Data is presented as  $\mu\text{M}$  of Cl or  $\mu\text{M}$  of Br. This approach would be similar to that of Adsorbable Organic Halides (AOX) [45]. The formation of smaller and volatile compounds, resulting from BPA's benzene ring opening, has been reported previously, with the formation of many known DBPs [17]. The decrease in EOX measured is a sign of poor recovery of smaller or volatile compounds using our selected approach, which is in agreement with our strategy of evaluating the different toxicity endpoints being related to the XBPA forms used in this study. Previous studies have also reported that drying steps included during solid-phase extraction result in over 98% loss in volatile disinfection by-products and inorganic species [61,62]. Since the fraction analysed corresponds to the extractable fraction, any purgeable components (e.g., chloroform) would not be monitored. In this setting we hypothesize that the increase in chemical oxidant concentration leads to BPA ring opening and formation of smaller volatile DBPs that are lost during extraction. Absolute recovery

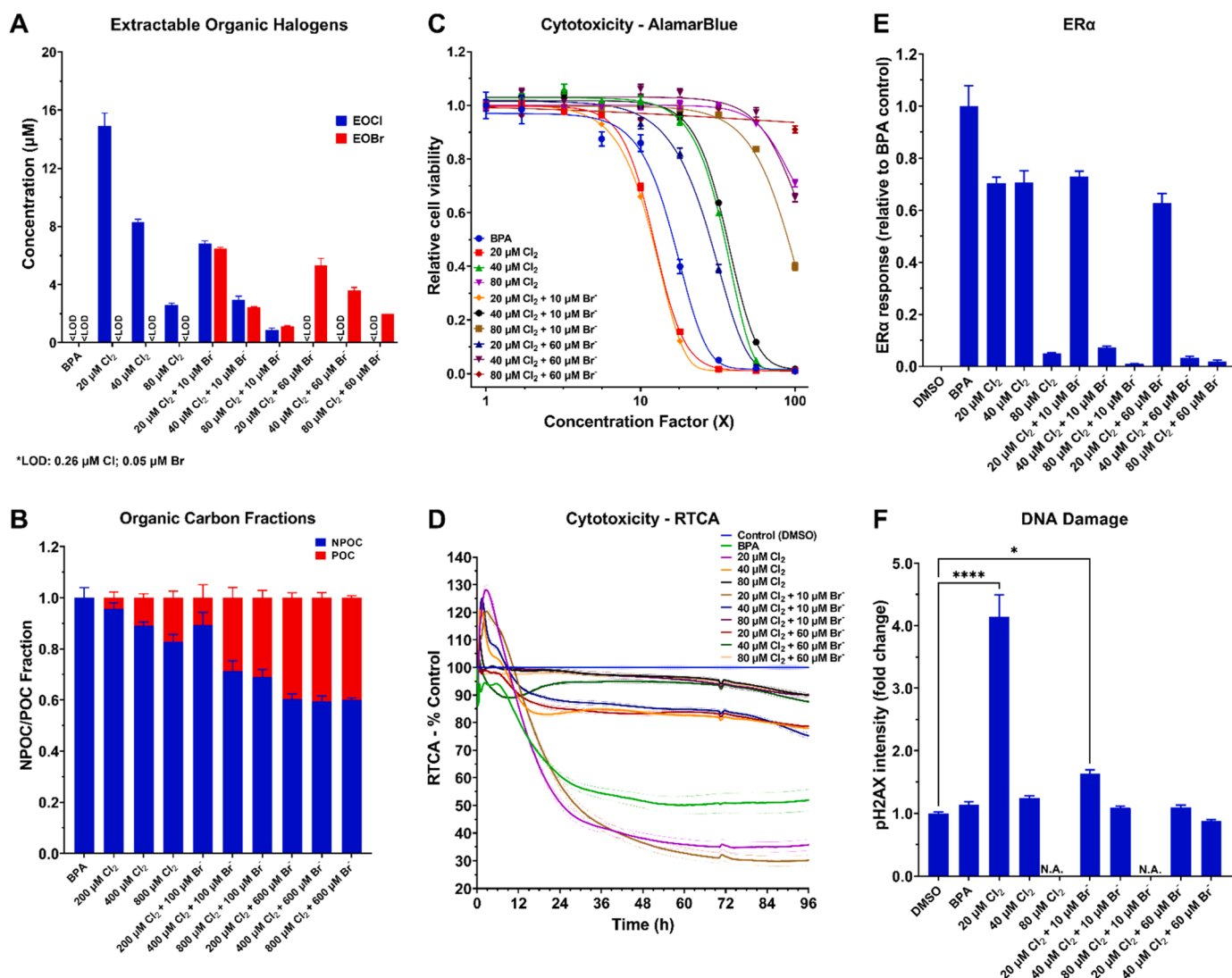


Fig. 4. Transformation and toxicity of BPA under simulated water chlorination in the presence of bromide. A) Extractable organic halogens (EOX),  $n = 3$ ; B) Organic carbon fractions (NPOC/POC),  $n = 3$ ; C) Cytotoxicity using cell viability assay (AlamarBlue); D) Cytotoxicity using RTCA assay,  $n = 6$ ; dotted lines represent measurement SEM; E) ER $\alpha$  activation using GeneBLazer assays,  $n = 5$ , error bars represent SEM; F) DNA Damage assay using pH2AX biomarker,  $n = 6$ , error bars represent SEM). \* denotes  $p < 0.05$ , \*\*\*\* denotes  $p < 0.0001$ ; from DMSO control using one-way ANOVA analysis.

for the 20 XBPA forms for which we had analytical standards were above 85% for all compounds looking at a spike recovery test at 200 ng/L ( $n = 5$ ), Figure S6. While many knowledge gaps still exist in the formation and toxicity of volatile DBPs [63], many studies focusing on their potential toxic effects are already available [64,65] and regulation or discussion about regulating such compounds are already common [66]. In our experimental design and multi-biomarker approach we have limited our testing to XBPA species and are not focused on smaller or volatile species.

Cytotoxicity of resulting extracts was also associated with the EOX concentration. Results showed that a greater incorporation of halogens to the BPA structure induced a lower  $EC_{50}$  value than the BPA control sample with 74.5% and 66.3% of added  $Cl_2$  incorporated as EOX for the samples with a  $Cl_2$ :BPA ratio of 2, with no bromine or 10  $\mu M$  bromide, respectively, Fig. 4C. Total EOX (EOCl + EOBr) for the same  $Cl_2$ :BPA ratio of 2 was similar across reactions with no bromine or 10  $\mu M$  bromide (14.90 and 13.26  $\mu M$ , respectively). The lower EOX value (5.30  $\mu M$ ) observed at 60  $\mu M$  bromide might be justified by similar reasons as discussed previously due to the reactivity of HOBr with phenols. A similar pattern was also observed for the real-time cell analysis experiments with monitoring of impedance, where the most toxic samples induced a rapid decrease in cellular impedance when compared to controls, Fig. 4D. RTCA analysis also shows that with experimental conditions used, cells are not able to recover from exposure with effects observed up to 96 h after exposure. This is also supported by real time monitoring of ROS as shown in later sections. Similar results were also found by another study which used impedance-based real time screening of BPA and other xenoestrogens as a potential endpoint that is complementary to traditional toxicity testing methods [67].

While chlorination of BPA leads to a significant effect on estrogen receptor activity with a reduction on the relative  $ER\alpha$  response for all conditions tested, Fig. 4E, this reduction was most significant with an increased  $Cl_2$ :BPA ratio and bromide concentration. Such observation is supported by previous studies [68,69] and the potential structural changes that chlorine induce in the BPA molecule [70]. Contrastingly to  $ER\alpha$  responses, effects on pH2AX, a biomarker for DNA damage, showed a significant increase for the two samples with the greater toxicity in AlamarBlue and RTCA assays. The pH2AX fold change over control was  $4.14 \pm 1.22$  for a  $Cl_2$ :BPA ratio of 2 without the presence of bromide and  $1.63 \pm 0.20$  in the presence of 10  $\mu M$  bromide, Fig. 4F. Increased genotoxic potential of compounds after chlorination has been demonstrated

in a plethora of studies using selected chemicals [52,71], and in the assessment of complex water and wastewater samples [72,73].

### 3.4. Selected XBPA cytotoxicity

Although different studies have focused on different toxicity endpoints of different halogenated forms of BPA [16], and others have evaluated the formation of different species under different conditions [2], a comprehensive multi-biomarker assessment of XBPA toxicity is still not available. This is especially critical considering the lack of information regarding the different isobaric species that are usually reported collectively in many previous studies as previously mentioned. Table 1 shows cytotoxicity  $EC_{50}$  values for three different exposure times (24, 48 and 72 h), dose-response curves for individual chemicals are presented on Figure S7–8. Comparing the toxicity observed for the complex mixture of the BPA chlorination samples and adding up each of their relative toxicity based on their general abundance in the mixture would indicate that the selected chemicals account for on average 65.3% of the total toxicity (range 30.9% to 81.5%), Table S5. However, this simplistic approach does not consider however any potential interactions these chemicals might have when present in a complex mixture.

While in the lack of standardized tests makes the direct comparison across different studies difficult, other major classes of small and volatile disinfection by-products such trihalomethanes (THMs), haloacetic acids (HAAs), haloacetonitriles (HANs), halonitromethanes (HNMs), haloacetamides (HAMs), and nitrosamines (NOAs) showed cytotoxicity  $EC_{50}$  values in the range of 29 to 1470  $\mu M$  towards HepG2 cells in a similar metabolic assay [74]. For that same study, most molecules showed a  $EC_{50}$  values above 100  $\mu M$ , except for dibromoacetonitrile (DBAN) at 29  $\mu M$ . Other studies also show a wide range in cytotoxicity for major classes of DBPs [42]. Other recently reported nitrogenous aromatic halogenated DBPs also presented greater  $EC_{50}$  values (~100–500  $\mu M$ ) than the ones we report here for XBPA (~20–90  $\mu M$ ) [75]. Cytotoxicity experiment also enabled the selection of a non-cytotoxic dose of 10  $\mu M$  for other experiments presented in this study ( $EC_{10}$  range for 20 halogenated compounds was 13 - 56  $\mu M$ ).

While there was no observable correlation between cytotoxicity  $EC_{50}$  values and  $ER\alpha$   $EC_{50}$  (Pearson  $r = 0.1390$ ,  $p = 0.548$ ), cytotoxicity at different exposure times showed strong correlations and statistically significant differences (Figure S9).  $EC_{50}$  values showed no statistically significant correlation with the number of Br, Cl or X (Br + Cl). A

**Table 1**  
Cytotoxicity and  $ER\alpha$   $EC_{50}$  values and 95% confidence intervals (CI) for BPA and XBPA.

| Chemical Name           | Cytotoxicity (AlamarBlue)   |             |                             |             |                             |             | $ER\alpha$ (GeneBLazer) |             |
|-------------------------|-----------------------------|-------------|-----------------------------|-------------|-----------------------------|-------------|-------------------------|-------------|
|                         | $EC_{50}$ -24 h ( $\mu M$ ) | 95% CI      | $EC_{50}$ -48 h ( $\mu M$ ) | 95% CI      | $EC_{50}$ -72 h ( $\mu M$ ) | 95% CI      | $EC_{50}$ (nM)          | 95% CI      |
| BPA                     | 145.4                       | 139.1-151.8 | 138.3                       | 123.3-153.3 | 136.5                       | 125.9-147.0 | 249.9                   | 239.8-260.0 |
| 2-Cl-BPA                | 55.5                        | 53.4-57.5   | 45.1                        | 44.3-45.9   | 45.9                        | 44.7-47.1   | 3697                    | 3434-3959   |
| 2,6-DiCl-BPA            | 83.8                        | 81.5-86.2   | 73.1                        | 72.1-74.0   | 77.5                        | 76.4-78.4   | 3162                    | 2659-3664   |
| 2,2'-DiCl-BPA           | 30.1                        | 29.1-31.0   | 25.0                        | 24.7-25.3   | 25.2                        | 24.8-25.6   | 4132                    | 4007-4256   |
| 2,2',6-TriCl-BPA        | 48.4                        | 46.5-50.3   | 40.6                        | 39.6-41.5   | 44.6                        | 43.7-45.5   | 13920                   | 13775-14064 |
| 2,2',6,6'-TetraCl-BPA   | 57.9                        | 55.6-60.1   | 47.3                        | 46.3-48.3   | 48.6                        | 43.5-53.7   | 18970                   | 18008-19931 |
| 2-Br-6-Cl-BPA           | 85.7                        | 83.1-88.2   | 51.6                        | 50.7-52.5   | 51.9                        | 50.0-53.8   | 40880                   | 19025-62734 |
| 2-Br-2'-Cl-BPA          | 34.0                        | 33.3-34.6   | 25.5                        | 24.9-26.0   | 25.7                        | 25.0-26.3   | 1781                    | 1720-1841   |
| 2-Br-2',6-DiCl-BPA      | 45.9                        | 44.9-46.9   | 40.0                        | 39.7-40.4   | 44.2                        | 43.6-44.8   | 3420                    | 3357-3482   |
| 2-Br-2',6'-DiCl-BPA     | 45.5                        | 43.9-47.1   | 40.2                        | 39.8-40.6   | 45.9                        | 44.6-47.2   | 4044                    | 3993-4094   |
| 2-Br-2',6,6'-TriCl-BPA  | 77.4                        | 74.9-79.8   | 47.6                        | 44.1-51.0   | 59.3                        | 58.0-60.6   | 1905                    | 1860-1949   |
| 2,2'-DiBr-6-Cl-BPA      | 42.1                        | 39.7-44.5   | 29.7                        | 29.0-30.3   | 36.6                        | 35.6-37.5   | 7706                    | 7345-8066   |
| 2,6-DiBr-2'-Cl-BPA      | 42.1                        | 41.6-42.5   | 28.8                        | 28.2-29.2   | 32.6                        | 31.6-33.5   | 1705                    | 1678-1731   |
| 2,2'-DiBr-6,6'-DiCl-BPA | 44.3                        | 43.0-45.6   | 37.9                        | 35.4-40.5   | 43.4                        | 41.3-45.5   | 1358                    | 1332-1383   |
| 2,6-DiBr-2',6'-DiCl-BPA | 48.2                        | 47.2-49.2   | 44.8                        | 44.2-45.3   | 47.3                        | 46.1-48.4   | 2759                    | 2681-2836   |
| 2,2',6-TriBr-6'-Cl-BPA  | 41.8                        | 40.9-42.7   | 40.7                        | 39.3-42.0   | 48.1                        | 45.6-50.5   | 1367                    | 1326-1407   |
| 2-Br-BPA                | 43.0                        | 41.8-44.2   | 37.4                        | 36.2-38.6   | 43.3                        | 42.5-44.1   | 3935                    | 3883-3986   |
| 2,6-DiBr-BPA            | 66.9                        | 65.6-68.2   | 46.7                        | 45.2-48.3   | 66.6                        | 65.4-67.8   | 3331                    | 3229-3432   |
| 2,2'-DiBr-BPA           | 22.2                        | 21.4-22.9   | 18.2                        | 17.3-18.9   | 24.2                        | 23.8-24.6   | 2191                    | 2138-2243   |
| 2,2',6-TriBr-BPA        | 36.4                        | 35.7-37.1   | 29.6                        | 25.8-33.4   | 42.4                        | 41.9-42.8   | 3372                    | 3343-3400   |
| 2,2',6,6'-TetraBr-BPA   | 44.4                        | 43.2-45.5   | 38.0                        | 37.7-38.4   | 44.7                        | 43.8-45.6   | 2916                    | 2806-3025   |

significant correlation observed only with the number of X atoms in the BPA ring positions 2 or 2' or only at position 2' (Pearson  $r = 0.605$ ,  $p = 0.003$ ; Pearson  $r = 0.562$ ,  $p = 0.008$ , respectively). Bromination or chlorination at other ring positions also showed no significant correlations. A multiple linear regression model using the number of Br, Cl atoms and the total number of atoms in the BPA ring positions 2 or 2' also showed that such parameters would be able to predict the observed cytotoxicity  $EC_{50}$  values ( $R [2] = 0.808$ ), Figure S10. A summary of the correlation analysis is presented on Figure S9.

### 3.5. Cell bioenergetics

While cytotoxicity is an important endpoint in toxicity evaluation, other assays might provide useful information about the underlying causes of reduced cell viability. Cell bioenergetics measurements are based on mitochondrial stress test assay using electron transport chain modulators. While this approach has been widely used in different fields, we also highlight its use in recent works related to the assessment of chemical pollutants and complex environmental mixtures [44,45,52,76,77]. Additionally, such triggers might also be observed at much lower concentrations providing a more sensitive way to monitor the potential deleterious effect of halogenated-BPA forms.

Upon exposure to BPA at different concentrations or XBPA forms all showed a significant impact on cellular respiration, maximal respiration, adenosine triphosphate (ATP) production, Fig. 5. All three parameters also showed strong Pearson correlation coefficients with observed cytotoxicity at different timepoints (24, 48 and 72 h), Pearson  $r > 0.5$ . Association with halogenation number or ring position were also similar to those observed for cytotoxicity analysis, Pearson  $r$  with 2 or 2' positions of 0.727 ( $p = 0.0001$ ),  $-0.853$  ( $p = 0.0001$ ) and

$-0.878$  ( $p = 0.0001$ ) for OCR change, ATP production and maximal respiration, respectively.

Bioenergetics data shows that many of the halogenated BPA forms have a significant effect of coupling efficiency, Fig. 5C. This was observed despite quantitative structure–activity relationship (QSAR) structure profiling would indicate that most compounds have an undefined concern for uncoupling of oxidative phosphorylation (OxPhos), with only 2,2',6,6'-TetraBr-BPA and 2,2',6,6'-TetraCl-BPA being listed as having a high concern for uncoupling of OxPhos, due to their predicted  $\log K_{ow} > 1.5$ . While an increasing degree of halogenation seems to have an increasing impact on the coupling efficiency, a clear pattern related to ring position and bromination or chlorination position was not observed. Although mitochondrial dysfunction has been reported previously with the exposure to BPA [78,79], little is known about the effects of XBPA, with the few studies available focusing on tetrahalogenated species [80,81].

### 3.6. Oxidative stress

While the monitoring of oxidative stress responses can be an early and sensitive indicator for the presence of chemical stressors in cells, many are the potential triggers of such effects [82]. In our work, all chemicals tested induced a significant change in the ROS, Fig. 6A. Observed changes in intracellular ROS showed the strongest correlations with observed cytotoxicity ( $EC_{50}$  - 24 h) when compared to other bioassay endpoints used in the work (Pearson  $r = -0.846$ ,  $p < 0.0001$ ). Oxidative stress has been reported as a marker of BPA toxicity both in vitro [78] and in vivo [83,84]. Studies with XBPA can be limited to few molecules [85], however, such previous studies generally support the hypothesis of a mitochondrial dependent oxidative stress response [80,

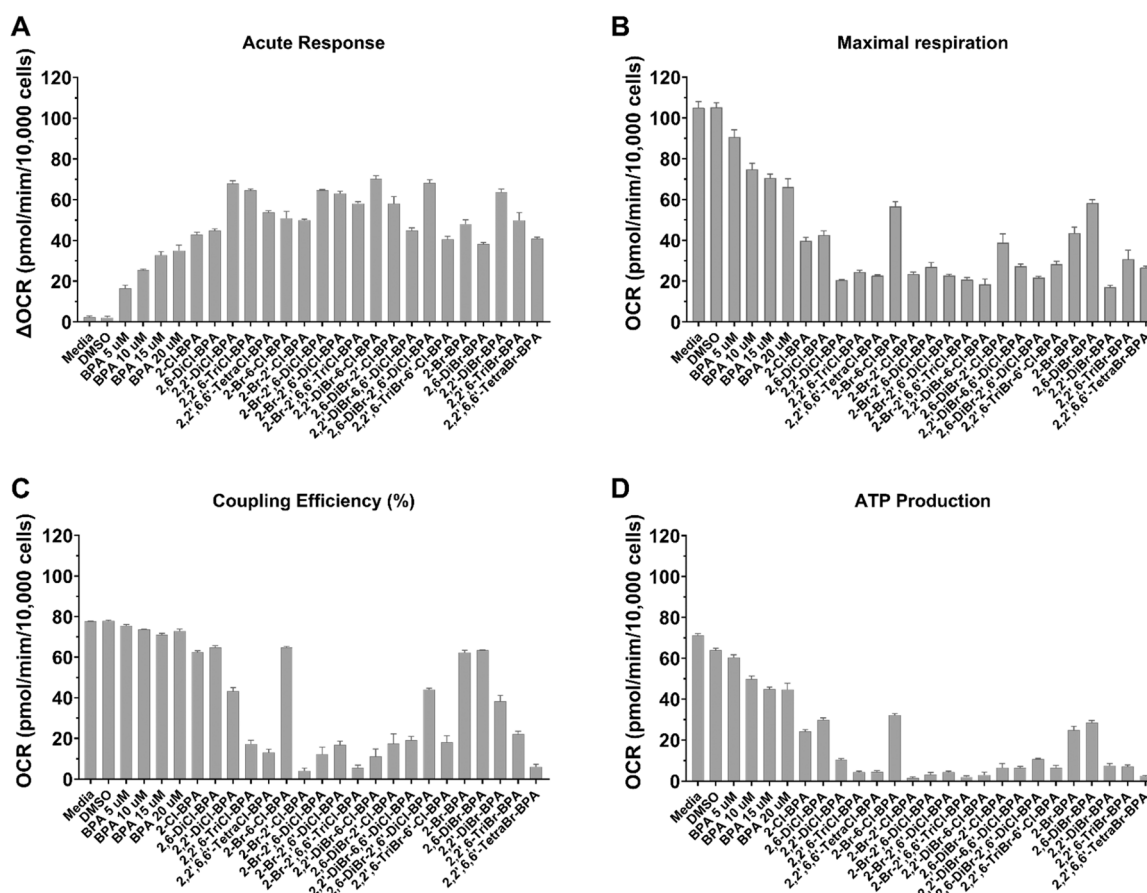
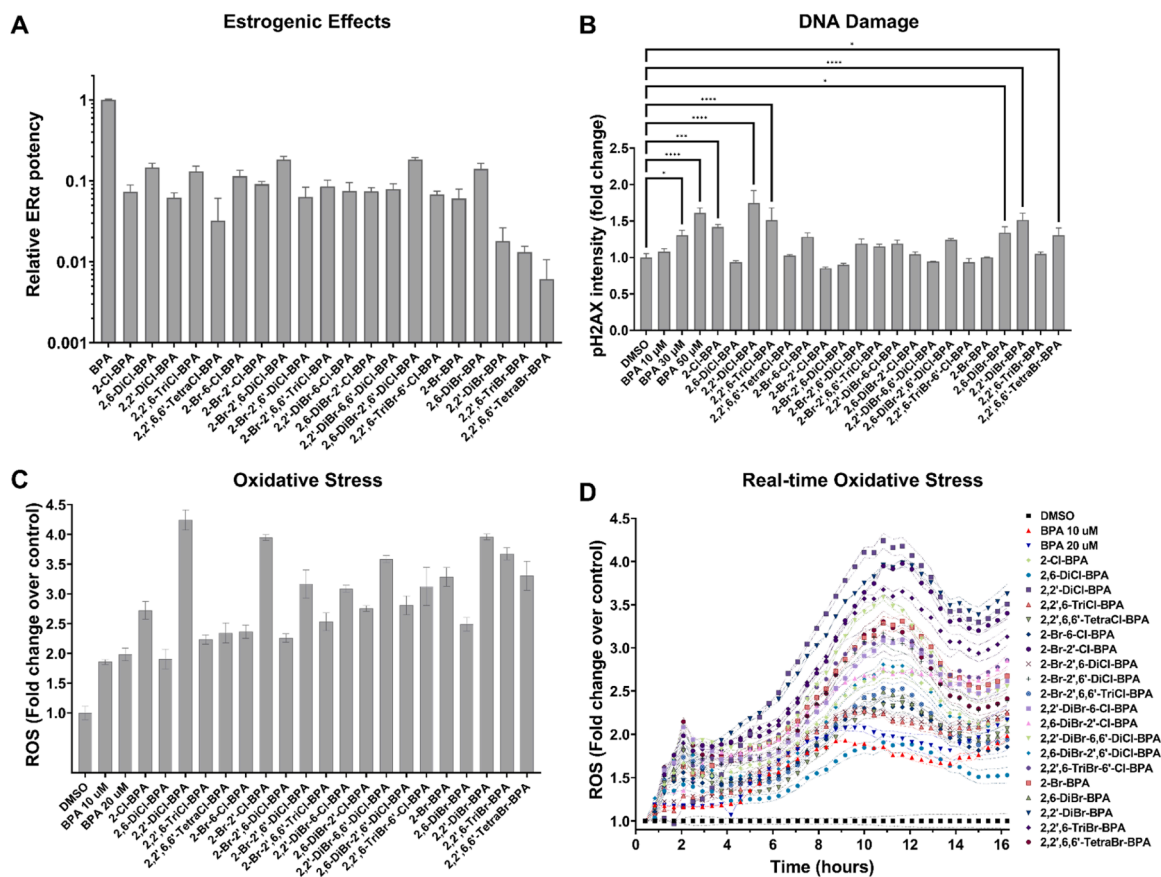


Fig. 5. Effects of XBPA (10 μM) on cellular bioenergetics. A) Mitochondrial stress test (MST) acute response; B) MST Maximal respiration; C) MST Coupling efficiency (%); D) MST ATP production. Data presented a mean  $\pm$  SEM ( $n = 6$ ).



**Fig. 6.** Effects of XBPA (10  $\mu\text{M}$ ) on different bioassay endpoints. A) Oxidative stress assay, monitoring of intracellular reactive oxygen species (ROS) using CellROX Green; exposure time of 11 h, all treatment conditions were statistically different from control ( $p < 0.05$ , from DMSO control using one-way ANOVA analysis); B) Real-time cell analysis of oxidative stress response using CellROX Green ( $n = 5$ ; dotted lines represent SEM); C) ER $\alpha$  relative potency; D) DNA damage assay using pH2AX biomarker ( $n = 6$ , error bars represent SEM). \* denotes  $p < 0.05$ , \*\* denotes  $p < 0.01$ , \*\*\* denotes  $p < 0.001$ , \*\*\*\* denotes  $p < 0.0001$ ; from DMSO control using one-way ANOVA analysis.

84]. Also supporting such observations of an increase in intracellular ROS species is an observed inhibition of SOD1 expression, Fig. 7D. Such inhibition of SOD1 expression was also previously demonstrated after BPA exposure [86]. Oxidative stress also exhibited a time dependent profile in RTCA analysis, with a peak being observed around 10 to 12 h post exposure, Fig. 6B. This timeline in observed effects also corresponds to the peak leading to changes in RTCA responses for cytotoxicity in water extracts (Fig. 4D) and for tests with individual compounds (data not shown).

### 3.7. Estrogen receptor $\alpha$ (ER $\alpha$ ) activation

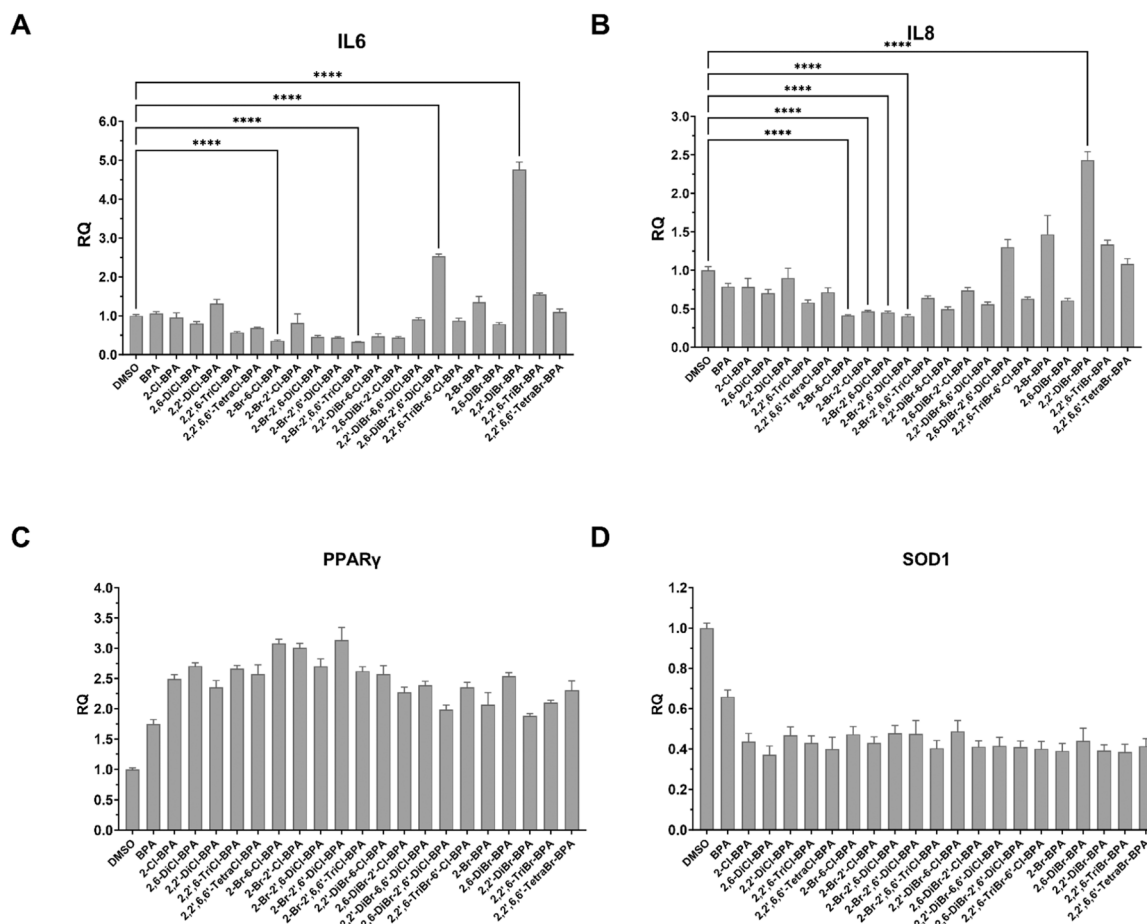
BPA is a very strong ER $\alpha$  binding molecule due to presence of the unhindered hydroxyl-groups positions in its structure being able to interact with sites of ER $\alpha$  receptor (site A E353/ R394 and site B H524) [87]. Most of the selected XBPA molecules showed significant lower ER $\alpha$  potency when compared to BPA ( $\sim 10 - 100$  x lower), Fig. 6C. This reduced activity is in line with QSAR structure profiling that indicated that all XBPA would still be predicted to be strong or very strong binders of ER $\alpha$  receptor, except for tetrahalogenated forms of BPA due to higher molecular weight (M.W. > 500) and/or the impairment of both OH groups by the four halogen atoms incorporated. This pattern was also previously observed in a work that studied the molecular recognition process of some halogenated BPA forms towards PPAR $\gamma$  and ER $\alpha$  receptors [88]. However, our observations are different from earlier studies that suggested stronger binding affinities for some chlorinated BPA species towards ER $\alpha$  [89–91]. Individual dose-response curves for XBPA chemicals using ER $\alpha$  GeneBLazer assay are presented on

Figure S11.

### 3.8. DNA damage

Although QSAR structure profiling showed no alerts for any of the studied XBPA forms, five of the XBPA had a small but still statistically significant increase in pH2AX intensity (2,2'-DiCl-BPA, 2,6-DiCl-BPA, 2,6-DiBr-BPA, 2,2'-DiBr-BPA and 2,2',6,6'-TetraBr-BPA), Fig. 6D. While previous studies have shown no effects of pH2AX for TBBPA [92], some data do suggest DNA damage in other assays and organisms [93, 94]. The effects observed for higher concentrations of BPA (i.e., 30 and 50  $\mu\text{M}$ ) were similar to those observed previously [92,95].

Although 2,6-DiCl-BPA and 2,2'-DiCl-BPA showed greater pH2AX fold change when compared to brominated counterparts 2,6-DiBr-BPA and 2,2'-DiBr-BPA, the  $4.14 \pm 1.21$  fold change observed in the chlorinated water sample (2:1 Cl $_2$ :BPA molar ratio in the absence of bromide, Fig. 4F) could not be solely explained by additive effects of the chlorinated BPA forms evaluated. Additionally, while the total EOX value observed for the 2:1 Cl $_2$ :BPA reaction with no bromide and with 10  $\mu\text{M}$  bromide was similar (14.90  $\mu\text{M}$  versus 13.26  $\mu\text{M}$ ) (Fig. 4A), DNA damage response was not equivalent for said conditions. This suggested that other forms not evaluated might be present or that potential synergistic effects among studied molecules might be at play. No associations were observed between DNA damage response and other endpoints evaluated in this study, except only a medium but not statistically significant association found with coupling efficiency (Pearson  $r = 0.313$ ,  $p = 0.168$ ). Similar responses with increased genotoxic effect for chlorinated over brominated forms were also observed for



**Fig. 7.** Relative gene expression analysis, XBPA concentration of 10  $\mu$ M. A) IL6; B) IL8; C) PPAR $\gamma$ , all treatment conditions were statistically different from control ( $p < 0.05$ , from DMSO control using one-way ANOVA analysis); D) SOD1, all treatment conditions were statistically different from control ( $p < 0.05$ , from DMSO control using one-way ANOVA analysis). Data presented a mean  $\pm$  SEM ( $n = 5$ ). \* \* \* \* denotes  $p < 0.0001$ ; from DMSO control using one-way ANOVA analysis.

halobenzoquinones, another class of potential water disinfection by-product, with similar structure-toxicity relationships for halogen atom positions as those observed for XBPA [96].

### 3.9. Inflammatory response and PPAR $\gamma$

Halogenation of BPA has been previously predicted to induce a reduction in ER $\alpha$  activity while contributing to increased PPAR $\gamma$  activity [88]. In our study, while BPA also showed a significant increase in gene expression for PPAR $\gamma$ , many XBPA forms showed an even greater overexpression of PPAR $\gamma$ , Fig. 7C. This increased effect towards PPAR $\gamma$  receptor is consistent with previous studies that used both modelling tools and in vitro testing for selected XBPA species [15,91,97]. Such observations are of importance since PPAR $\gamma$  has been implicated in many human metabolic diseases [98] with its dysfunction associated to conditions such as obesity and diabetes [99]. Expression of proinflammatory cytokines IL6 and IL8 was also affected by the exposure of selected XBPA, with IL6 significantly overexpressed by 2,6-DiBr-2',6'-DiCl-BPA and 2,2'-DiBr-BPA and IL8 overexpressed in 2,2'-DiBr-BPA sample, Fig. 7A and B. Some XBPA forms also were responsible for a significant inhibition of IL6 and IL8 expression. In vivo studies with BPA and TCBPA also showed alteration in the expression profile of cytokines [84,100].

## 4. Conclusions

Using OSPE-LC-IM-HRMS we showed that the separation of multiple isomeric pairs of XBPA is possible with total analysis time of 10 min,

including sample concentration. Use of three orthogonal separation modes (RT, CCS and  $m/z$ ) showed that different halogenated forms of BPA are generated under different chlorination conditions, with or without the presence of bromide ions, including many Br $_x$ Cl $_y$ -BPA species that were previously weakly studied.

While previous studies have demonstrated the formation of a diverse set of XBPA, few have focused on understanding the potential roles of halogenation position on BPA rings and its impact on cellular toxicity. A multi-biomarker approach to comprehensively study toxic effects of different XBPA species reveals that impacts on cytotoxicity and cellular bioenergetics cannot be correlated solely with the number of Br, Cl or X (Br + Cl). A significant correlation was observed only with the number of X atoms in the BPA ring positions 2 or 2' or only at position 2'. Bromination or chlorination at other ring positions also showed no significant correlations. Halogenation of BPA resulted in reduced activation of ER $\alpha$ , which can be associated with the hindrance of BPA hydroxyl groups by halogen atoms and increased molecular weight of transformation products. Selected XBPA species also showed significant impacts on PPAR $\gamma$  and inflammatory response (IL6 and IL8 expression). However, DNA damage observed in chlorinated water samples could not be explained by additive effects of examined XBPA forms only.

## Statement of environmental implication

BPA is a widely used polymer additive with current reports implicating its leaching from plethora of materials leading to widespread environmental occurrence, including in humans. Halogenated forms resulting from water chlorination can lead to increased toxicity and

different biological effects. Here we present a novel approach to differentiate isomeric XBPA forms while using a multi-biomarker approach to comprehensively study the different toxic effects of such species.

### CRedit authorship contribution statement

**Marques dos Santos Mauricius:** Conceptualization, Formal analysis, Investigation, Methodology, Visualization, Writing – review & editing. **Thomas Mikael:** Investigation, Writing – review & editing. **Gallard Hervé:** Conceptualization, Writing – review & editing. **Li Caixia:** Investigation, Writing – review & editing. **Jia Shenglan:** Investigation, Writing – review & editing. **Snyder Shane:** Conceptualization, Methodology, Supervision, Writing – original draft. **Croué Jean-Philippe:** Conceptualization, Writing – review & editing. **Carato Pascal:** Conceptualization, Resources, Writing – review & editing.

### Declaration of Competing Interest

The authors declare the following financial interests/personal relationships which may be considered as potential competing interests: Shane Allen Snyder reports financial support was provided by National Research Foundation, Singapore. Shane Allen Snyder reports financial support was provided by PUB Singapore's National Water Agency. Shane Allen Snyder reports equipment, drugs, or supplies was provided by Agilent Technologies Inc.

### Data Availability

Data will be made available on request.

### Acknowledgments

This work is funded by National Research Foundation, Singapore, and PUB, under its RIE2025 USS (Water) Centre of Excellence (CoE) programme – RIE2025-CoE/NEWRI). Authors acknowledge and are thankful to Agilent Technologies for xCELLigence RTCA instrument and support through a research collaboration agreement (RCA-2019-0349). Authors are thankful to Mdm. Ohnmar for assistance with halogenated products of BPA importation and customs processes.

### Appendix A. Supporting information

Supplementary data associated with this article can be found in the online version at [doi:10.1016/j.jhazmat.2023.133229](https://doi.org/10.1016/j.jhazmat.2023.133229).

### References

- [1] Kadasala, N.R., Narayanan, B., Liu, Y., 2016. International trade regulations on BPA: global health and economic implications. *Asian Dev Policy Rev* 4 (4), 134–142.
- [2] Li, J., He, J., Aziz, M.T., Song, X., Zhang, Y., Niu, Z., 2021. Iodide promotes bisphenol A (BPA) halogenation during chlorination: evidence from 30 X-BPAs (X = Cl, Br, and I). *J Hazard Mater* 414, 125461.
- [3] Jiang, D., Chen, W.-Q., Zeng, X., Tang, L., 2018. Dynamic stocks and flows analysis of bisphenol A (BPA) in China: 2000–2014. *Environ Sci Technol* 52 (6), 3706–3715.
- [4] Corrales, J., Kristofco, L.A., Steele, W.B., Yates, B.S., Breed, C.S., Williams, E.S., et al., 2015. Global assessment of bisphenol a in the environment: review and analysis of its occurrence and bioaccumulation. *Dose-Response* 13 (3), 1559325815598308.
- [5] Wang, L., Zhang, Y., Liu, Y., Gong, X., Zhang, T., Sun, H., 2019. Widespread occurrence of bisphenol a in daily clothes and its high exposure risk in humans. *Environ Sci Technol* 53 (12), 7095–7102.
- [6] Muhamad, M.S., Salim, M.R., Lau, W.J., Yusop, Z., 2016. A review on bisphenol A occurrences, health effects and treatment process via membrane technology for drinking water. *Environ Sci Pollut Res* 23 (12), 11549–11567.
- [7] da Silva Costa, R., Sainara Maia Fernandes, T., de Sousa Almeida, E., Tomé Oliveira, J., Carvalho Guedes, J.A., Julião Zocolo, G., et al., 2021. Potential risk of BPA and phthalates in commercial water bottles: a minireview. *J Water Health* 19 (3), 411–435.
- [8] Albouy, M., Deceuninck, Y., Migeot, V., Dumas, M., Dupuis, A., Venisse, N., et al., 2023. Characterization of pregnant women exposure to halogenated parabens and bisphenols through water consumption. *J Hazard Mater* 448, 130945.
- [9] Jeon, G.W., 2022. Bisphenol A leaching from polycarbonate baby bottles into baby food causes potential health issues. *Clin Exp Pediatr* 65 (9), 450–452.
- [10] Manikkam, M., Tracey, R., Guerrero-Bosagna, C., Skinner, M.K., 2013. Plastics derived endocrine disruptors (BPA, DEHP and DBP) induce epigenetic transgenerational inheritance of obesity, reproductive disease and sperm epimutations. *PLOS ONE* 8 (1), e55387.
- [11] LaKind, J.S., Goodman, M., Mattison, D.R., 2014. Bisphenol A and indicators of obesity, glucose metabolism/type 2 diabetes and cardiovascular disease: A systematic review of epidemiologic research. *Crit Rev Toxicol* 44 (2), 121–150.
- [12] Pelch, K., Wignall, J.A., Goldstone, A.E., Ross, P.K., Blain, R.B., Shapiro, A.J., et al., 2019. A scoping review of the health and toxicological activity of bisphenol A (BPA) structural analogues and functional alternatives. *Toxicology* 424, 152235.
- [13] Andra, S.S., Charisiadis, P., Arora, M., van Vliet-Ostapchouk, J.V., Makris, K.C., 2015. Biomonitoring of human exposures to chlorinated derivatives and structural analogs of bisphenol A. *Environ Int* 85, 352–379.
- [14] Riu, A., McCollum, C.W., Pinto, C.L., Grimaldi, M., Hillenweck, A., Perdu, E., et al., 2014. Halogenated bisphenol-A analogs act as obesogens in zebrafish larvae (*Danio rerio*). *Toxicol Sci* 139 (1), 48–58.
- [15] Riu, A., Grimaldi, M., le Maire, A., Bey, G., Phillips, K., Boulahtouf, A., et al., 2011. Peroxisome proliferator-activated receptor  $\gamma$  is a target for halogenated analogs of bisphenol A. *Environ Health Perspect* 119 (9), 1227–1232.
- [16] Plattard, N., Dupuis, A., Migeot, V., Haddad, S., Venisse, N., 2021. An overview of the literature on emerging pollutants: chlorinated derivatives of Bisphenol A (ClxBPA). *Environ Int* 153, 106547.
- [17] Li, C., Wang, Z., Yang, Y.J., Liu, J., Mao, X., Zhang, Y., 2015. Transformation of bisphenol A in water distribution systems: a pilot-scale study. *Chemosphere* 125, 86–93.
- [18] Dumas, M., Rouillon, S., Venisse, N., Nadeau, C., Pierre Eugene, P., Farce, A., et al., 2018. Chlorinated and brominated bisphenol A derivatives: synthesis, characterization and determination in water samples. *Chemosphere* 213, 434–442.
- [19] Dorival-García, N., Zafra-Gómez, A., Navalón, A., Vilchez, J.L., 2012. Analysis of bisphenol A and its chlorinated derivatives in sewage sludge samples. comparison of the efficiency of three extraction techniques. *J Chromatogr A* 1253, 1–10.
- [20] Li, A., Zhuang, T., Shi, W., Liang, Y., Liao, C., Song, M., et al., 2020. Serum concentration of bisphenol analogues in pregnant women in China. *Sci Total Environ* 707, 136100.
- [21] Hu, C., Schöttker, B., Venisse, N., Limousi, F., Saulnier, P.J., Albouy-Llaty, M., et al., 2019. Chlorinated derivatives of bisphenol a and occurrence of myocardial infarction in patients with type 2 diabetes: nested case-control studies in two european cohorts. *Environ Sci Technol* 53 (16), 9876–9883.
- [22] Vela-Soria, F., Ballesteros, O., Camino-Sánchez, F.J., Zafra-Gómez, A., Ballesteros, L., Navalón, A., 2015. Matrix solid phase dispersion for the extraction of selected endocrine disrupting chemicals from human placental tissue prior to UHPLC-MS/MS analysis. *Microchem J* 118, 32–39.
- [23] Niu, Y., Wang, B., Yang, R., Wu, Y., Zhao, Y., Li, C., et al., 2021. Bisphenol analogues and their chlorinated derivatives in breast milk in china: occurrence and exposure assessment. *J Agric Food Chem* 69 (4), 1391–1397.
- [24] Richardson, S.D., Fasano, F., Ellington, J.J., Crumley, F.G., Buettner, K.M., Evans, J.J., et al., 2008. Occurrence and mammalian cell toxicity of iodinated disinfection byproducts in drinking water. *Environ Sci Technol* 42 (22), 8330–8338.
- [25] Fan, Z., Hu, J., An, W., Yang, M., 2013. Detection and occurrence of chlorinated byproducts of bisphenol a, nonylphenol, and estrogens in drinking water of China: comparison to the parent compounds. *Environ Sci Technol* 47 (19), 10841–10850.
- [26] Chen, M., Fan, Z., Zhao, F., Gao, F., Mu, D., Zhou, Y., et al., 2016. Occurrence and maternal transfer of chlorinated bisphenol A and nonylphenol in pregnant women and their matching embryos. *Environ Sci Technol* 50 (2), 970–977.
- [27] Zhou, Y., Chen, M., Zhao, F., Mu, D., Zhang, Z., Hu, J., 2015. Ubiquitous occurrence of chlorinated byproducts of bisphenol a and nonylphenol in bleached food contacting papers and their implications for human exposure. *Environ Sci Technol* 49 (12), 7218–7226.
- [28] Zheng, S., Shi, J., Zhang, J., Yang, Y., Hu, J., Shao, B., 2018. Identification of the disinfection byproducts of bisphenol S and the disrupting effect on peroxisome proliferator-activated receptor gamma (PPAR $\gamma$ ) induced by chlorination. *Water Res* 132, 167–176.
- [29] McDaniel, E.W., Martin, D.W., Barnes, W.S., 1962. Drift tube-mass spectrometer for studies of low-energy ion-molecule reactions. *Rev Sci Instrum* 33 (1), 2–7.
- [30] Lanucara, F., Holman, S.W., Gray, C.J., Eyers, C.E., 2014. The power of ion mobility-mass spectrometry for structural characterization and the study of conformational dynamics. *Nat Chem* 6 (4), 281–294.
- [31] May, J.C., Goodwin, C.R., Lareau, N.M., Leapfrog, K.L., Morris, C.B., Kurulugama, R.T., et al., 2014. Conformational ordering of biomolecules in the gas phase: nitrogen collision cross sections measured on a prototype high resolution drift tube ion mobility-mass spectrometer. *Anal Chem* 86 (4), 2107–2116.
- [32] Ross, D.H., Xu, L., 2021. Determination of drugs and drug metabolites by ion mobility-mass spectrometry: a review. *Anal Chim Acta* 1154, 338270.

- [33] Skeene, K., Khatri, K., Soloviev, Z., Laphorn, C., 2021. Current status and future prospects for ion-mobility mass spectrometry in the biopharmaceutical industry. *Biochim Et Biophys Acta (BBA) - Proteins Proteom* 1869 (12), 140697.
- [34] Delafield, D.G., Lu, G., Kaminsky, C.J., Li, L., 2022. High-end ion mobility mass spectrometry: a current review of analytical capacity in omics applications and structural investigations. *TrAC Trends Anal Chem* 157, 116761.
- [35] Dodds, J.N., Hopkins, Z.R., Knappe, D.R.U., Baker, E.S., 2020. Rapid characterization of per- and polyfluoroalkyl substances (PFAS) by ion mobility spectrometry-mass spectrometry (IMS-MS). *Anal Chem* 92 (6), 4427–4435.
- [36] Foster, M., Rainey, M., Watson, C., Dodds, J.N., Kirkwood, K.I., Fernández, F.M., et al., 2022. Uncovering PFAS and other xenobiotics in the dark metabolome using ion mobility spectrometry, mass defect analysis, and machine learning. *Environ Sci Technol* 56 (12), 9133–9143.
- [37] Valdiviezo, A., Aly, N.A., Luo, Y.-S., Cordova, A., Casillas, G., Foster, M., et al., 2022. Analysis of per- and polyfluoroalkyl substances in Houston Ship Channel and Galveston Bay following a large-scale industrial fire using ion-mobility-spectrometry-mass spectrometry. *J Environ Sci* 115, 350–362.
- [38] Stephan, S., Hippler, J., Köhler, T., Deeb, A.A., Schmidt, T.C., Schmitz, O.J., 2016. Contaminant screening of wastewater with HPLC-IM-qTOF-MS and LC+LC-IM-qTOF-MS using a CCS database. *Anal Bioanal Chem* 408 (24), 6545–6555.
- [39] Belova, L., Celma, A., Van Haesendonck, G., Lemièrre, F., Sancho, J.V., Covaci, A., et al., 2022. Revealing the differences in collision cross section values of small organic molecules acquired by different instrumental designs and prediction models. *Anal Chim Acta* 1229, 340361.
- [40] Luo, Y.-S., Chen, Z., Hsieh, N.-H., Lin, T.-E., 2022. Chemical and biological assessments of environmental mixtures: a review of current trends, advances, and future perspectives. *J Hazard Mater* 432, 128658.
- [41] Zhang, X., Romm, M., Zheng, X., Zink, E.M., Kim, Y.-M., Burnum-Johnson, K.E., et al., 2016. SPE-IMS-MS: An automated platform for sub-sixty second surveillance of endogenous metabolites and xenobiotics in biofluids. *Clin Mass Spectrom* 2, 1–10.
- [42] Wagner, E.D., Plewa, M.J., 2017. CHO cell cytotoxicity and genotoxicity analyses of disinfection by-products: an updated review. *J Environ Sci* 58, 64–76.
- [43] Jia, S., Li, C., Fang, M., Marques Dos Santos, M., Snyder, S.A., 2022. Non-targeted metabolomics revealing the effects of bisphenol analogues on human liver cancer cells. *Chemosphere*, 134088.
- [44] Marques dos Santos, M., Tan Pei Fei, M., Li, C., Jia, S., Snyder, S.A., 2022. Cell-line and culture model specific responses to organic contaminants in house dust: cell bioenergetics, oxidative stress, and inflammation endpoints. *Environ Int* 167, 107403.
- [45] Wang, Y., Marques dos Santos, M., Ding, X., Labanowski, J., Gombert, B., Snyder, S.A., et al., 2021. Impact of EFOM in the elimination of PPCPs by UV/chlorine: radical chemistry and toxicity bioassays. *Water Res* 204, 117634.
- [46] Jin, S.-P., Li, Z., Choi, E.K., Lee, S., Kim, Y.K., Seo, E.Y., et al., 2018. Urban particulate matter in air pollution penetrates into the barrier-disrupted skin and produces ROS-dependent cutaneous inflammatory response in vivo. *J Dermatol Sci* 91 (2), 175–183.
- [47] Galloway, T.S., Brown, R.J., Browne, M.A., Dissanayake, A., Lowe, D., Jones, M. B., et al., 2004. Approach to environmental assessment. *Environ Sci Technol* 38 (6), 1723–1731.
- [48] Song, P., Jiang, N., Zhang, K., Li, X., Li, N., Zhang, Y., et al., 2022. Ecotoxicological evaluation of zebrafish liver (Danio rerio) induced by dibutyl phthalate. *J Hazard Mater* 425, 128027.
- [49] Marques dos Santos, M., Snyder, S.A., 2023. Occurrence of polymer additives 1,3-diphenylguanidine (DPG), N-(1,3-dimethylbutyl)-n'-phenyl-1,4-benzenediamine (6PPD), and chlorinated byproducts in drinking water: contribution from plumbing polymer materials. *Environ Sci Technol Lett*.
- [50] Benotti, M.J., Trenholm, R.A., Vanderford, B.J., Holady, J.C., Stanford, B.D., Snyder, S.A., 2009. Pharmaceuticals and endocrine disrupting compounds in U.S. drinking water. *Environ Sci Technol* 43 (3), 597–603.
- [51] Le, H.H., Carlson, E.M., Chua, J.P., Belcher, S.M., 2008. Bisphenol A is released from polycarbonate drinking bottles and mimics the neurotoxic actions of estrogen in developing cerebellar neurons. *Toxicol Lett* 176 (2), 149–156.
- [52] Marques dos Santos, M., Cheriaux, C., Jia, S., Thomas, M., Gallard, H., Croué, J.-P., et al., 2022. Genotoxic effects of chlorinated disinfection by-products of 1,3-diphenylguanidine (DPG): cell-based in-vitro testing and formation potential during water disinfection. *J Hazard Mater* 436, 129114.
- [53] Kristiana, I., Lethom, A., Joll, C., Heitz, A., 2014. To add or not to add: the use of quenching agents for the analysis of disinfection by-products in water samples. *Water Res* 59, 90–98.
- [54] Li, J., Chen, J., Zhang, Z., Liang, X., 2023. Impact of prevalent chlorine quenchers on phenolic disinfection byproducts in drinking water and potential reaction mechanisms. *Sci Total Environ* 871, 161971.
- [55] Bilbao, A., Gibbons, B.C., Stow, S.M., Kyle, J.E., Bloodsworth, K.J., Payne, S.H., et al., 2022. A preprocessing tool for enhanced ion mobility-mass spectrometry-based omics workflows. *J Proteome Res* 21 (3), 798–807.
- [56] Marques dos Santos, M., Hoppe-Jones, C., Snyder, S.A., 2019. DEET occurrence in wastewaters: seasonal, spatial and diurnal variability - mismatches between consumption data and environmental detection. *Environ Int* 132, 105038.
- [57] Gallard, H., Leclercq, A., Croué, J.-P., 2004. Chlorination of bisphenol A: kinetics and by-products formation. *Chemosphere* 56 (5), 465–473.
- [58] Criquet, J., Rodriguez, E.M., Allard, S., Wellauer, S., Salhi, E., Joll, C.A., et al., 2015. Reaction of bromine and chlorine with phenolic compounds and natural organic matter extracts – electrophilic aromatic substitution and oxidation. *Water Res* 85, 476–486.
- [59] Acero, J.L., Piriou, P., von Gunten, U., 2005. Kinetics and mechanisms of formation of bromophenols during drinking water chlorination: assessment of taste and odor development. *Water Res* 39 (13), 2979–2993.
- [60] Han, J., Zhang, X., Jiang, J., Li, W., 2021. How much of the total organic halogen and developmental toxicity of chlorinated drinking water might be attributed to aromatic halogenated DBPs? *Environ Sci Technol* 55 (9), 5906–5916.
- [61] Zhong, Y., Gan, W., Du, Y., Huang, H., Wu, Q., Xiang, Y., et al., 2019. Disinfection byproducts and their toxicity in wastewater effluents treated by the mixing oxidant of ClO<sub>2</sub>/Cl<sub>2</sub>. *Water Res* 162, 471–481.
- [62] Han, J., Zhang, X., 2018. Evaluating the comparative toxicity of DBP mixtures from different disinfection scenarios: a new approach by combining freeze-drying or rotoevaporation with a marine polychaete bioassay. *Environ Sci Technol* 52 (18), 10552–10561.
- [63] Li, X.-F., Mitch, W.A., 2018. Drinking water disinfection byproducts (DBPs) and human health effects: multidisciplinary challenges and opportunities. *Environ Sci Technol* 52 (4), 1681–1689.
- [64] Boorman, G.A., 1999. Drinking water disinfection byproducts: review and approach to toxicity evaluation. *Environ Health Perspect* 107 (Suppl 1 (Suppl 1)), 207–217.
- [65] Zhang, S.-h, Miao, D.-y, Tan, L., Liu, A.-l, Lu, W.-q, 2016. Comparative cytotoxic and genotoxic potential of 13 drinking water disinfection by-products using a microplate-based cytotoxicity assay and a developed SOS/umu assay. *Mutagenesis* 31 (1), 35–41.
- [66] Richardson, S.D., Plewa, M.J., 2020. To regulate or not to regulate? What to do with more toxic disinfection by-products? *J Environ Chem Eng* 8 (4), 103939.
- [67] Pupinyo, N., D'Costa, C., Heiskanen, A., Laiwattanapaisal, W., Emnéus, J., 2022. Impedance-based e-screen cell biosensor for the real-time screening of xenoestrogenic compounds. *ACS EST Water* 2 (3), 446–456.
- [68] Lee, B.-C., Kamata, M., Akatsuka, Y., Takeda, M., Ohno, K., Kamei, T., et al., 2004. Effects of chlorine on the decrease of estrogenic chemicals. *Water Res* 38 (3), 733–739.
- [69] Bourgin, M., Bichon, E., Antignac, J.-P., Monteau, F., Leroy, G., Barritaud, L., et al., 2013. Chlorination of bisphenol A: Non-targeted screening for the identification of transformation products and assessment of estrogenicity in generated water. *Chemosphere* 93 (11), 2814–2822.
- [70] Schultz, T.W., Sinks, G.D., Cronin, M.T.D., 2002. Structure-activity relationships for gene activation oestrogenicity: Evaluation of a diverse set of aromatic chemicals. *Environ Toxicol* 17 (1), 14–23.
- [71] Lan, J., Rahman, S.M., Gou, N., Jiang, T., Plewa, M.J., Alshawabkeh, A., et al., 2018. Genotoxicity assessment of drinking water disinfection byproducts by DNA damage and repair pathway profiling analysis. *Environ Sci Technol* 52 (11), 6565–6575.
- [72] Zhang, A., Jia, A., Park, M., Li, Y., Snyder, S.A., 2019. Genotoxicity assay and potential byproduct identification during different UV-based water treatment processes. *Chemosphere* 217, 176–182.
- [73] Jia, A., Escher, B.I., Leusch, F.D.L., Tang, J.Y.M., Prochazka, E., Dong, B., et al., 2015. In vitro bioassays to evaluate complex chemical mixtures in recycled water. *Water Res* 80, 1–11.
- [74] Kajumba, G.W., Bokota, R.E., Attene-Ramos, M., Marti, E.J., 2022. Evaluation of disinfection byproducts for their ability to affect mitochondrial function. *J Environ Sci* 117, 295–304.
- [75] Hu, S., Kaw, H.Y., Zhu, L., Wang, W., 2022. Formation and cytotoxicity of halophenylacetamides: a new group of nitrogenous aromatic halogenated disinfection byproducts in drinking water. *Environ Sci Technol* 56 (5), 3181–3192.
- [76] Jia, S., Li, C., Fang, M., Marques Dos Santos, M., Snyder, S.A., 2022. Non-targeted metabolomics revealing the effects of bisphenol analogues on human liver cancer cells. *Chemosphere* 297, 134088.
- [77] Wang, Y., Xiang, Y., Marques dos Santos, M., Wei, G., Jiang, B., Snyder, S., et al., 2023. UV/chlorine and chlorination of effluent organic matter fractions: tracing nitrogenous DBPs using FT-ICR mass spectrometry. *Water Res* 231, 119646.
- [78] Barbonetti, A., Castellini, C., Di Giammarco, N., Santilli, G., Francavilla, S., Francavilla, F., 2016. In vitro exposure of human spermatozoa to bisphenol A induces pro-oxidative/apoptotic mitochondrial dysfunction. *Reprod Toxicol* 66, 61–67.
- [79] Khan, S., Beigh, S., Chaudhari, B.P., Sharma, S., Aliul Hasan Abdi, S., Ahmad, S., et al., 2016. Mitochondrial dysfunction induced by Bisphenol A is a factor of its hepatotoxicity in rats. *Environ Toxicol* 31 (12), 1922–1934.
- [80] Jia, X., Yan, R., Lin, H., Liu, Z., Shen, L., Yang, H., et al., 2022. TBBPA and its alternative TCBPA induced ROS-dependent mitochondria-mediated apoptosis in the liver of Rana nigromaculata. *Environ Pollut* 297, 118791.
- [81] Bowen, C., Childers, G., Perry, C., Martin, N., McPherson, C.A., Lauten, T., et al., 2020. Mitochondrial-related effects of pentabromophenol, tetrabromobisphenol A, and triphenyl phosphate on murine BV-2 microglia cells. *Chemosphere* 255, 126919.
- [82] Escher, B.I., van Daele, C., Dutt, M., Tang, J.Y.M., Altenburger, R., 2013. Most oxidative stress response in water samples comes from unknown chemicals: the need for effect-based water quality trigger values. *Environ Sci Technol* 47 (13), 7002–7011.
- [83] Bindhumol, V., Chitra, K.C., Mathur, P.P., 2003. Bisphenol A induces reactive oxygen species generation in the liver of male rats. *Toxicology* 188 (2), 117–124.
- [84] Wang, K., Zhao, Z., Ji, W., 2019. Bisphenol A induces apoptosis, oxidative stress and inflammatory response in colon and liver of mice in a mitochondria-dependent manner. *Biomed Pharmacother* 117, 109182.

- [85] Zhang, X., Zhang, Y., Ji, Z., Wang, F., Zhang, L., Song, M., et al., 2020. Oxidative damage mechanism in *Saccharomyces cerevisiae* cells exposed to tetrachlorobisphenol A. *Environ Toxicol Pharmacol* 80, 103507.
- [86] Li, Y., Dong, Z., Liu, S., Gao, F., Zhang, J., Peng, Z., et al., 2022. Astaxanthin improves the development of the follicles and oocytes through alleviating oxidative stress induced by BPA in cultured follicles. *Sci Rep* 12 (1), 7853.
- [87] Gallegos Saliner, A., Amat, L., Carbó-Dorca, R., Schultz, T.W., Cronin, M.T.D., 2003. Molecular quantum similarity analysis of estrogenic activity. *J Chem Inf Comput Sci* 43 (4), 1166–1176.
- [88] Zhuang, S., Zhang, C., Liu, W., 2014. Atomic insights into distinct hormonal activities of bisphenol a analogues toward PPAR $\gamma$  and ER $\alpha$  receptors. *Chem Res Toxicol* 27 (10), 1769–1779.
- [89] Kuruto-Niwa, R., Terao, Y., Nozawa, R., 2002. Identification of estrogenic activity of chlorinated bisphenol A using a GFP expression system. *Environ Toxicol Pharmacol* 12 (1), 27–35.
- [90] Takemura, H., Ma, J., Sayama, K., Terao, Y., Zhu, B.T., Shimoi, K., 2005. In vitro and in vivo estrogenic activity of chlorinated derivatives of bisphenol A. *Toxicology* 207 (2), 215–221.
- [91] Riu, A., le Maire, A., Grimaldi, M., Audebert, M., Hillenweck, A., Bourguet, W., et al., 2011. Characterization of novel ligands of ER $\alpha$ , ER $\beta$ , and PPAR $\gamma$ : the case of halogenated bisphenol A and their conjugated metabolites. *Toxicol Sci* 122 (2), 372–382.
- [92] Quesnot, N., Rondel, K., Audebert, M., Martinais, S., Glaise, D., Morel, F., et al., 2016. Evaluation of genotoxicity using automated detection of  $\gamma$ H2AX in metabolically competent HepaRG cells. *Mutagenesis* 31 (1), 43–50.
- [93] Bearr, J.S., Stapleton, H.M., Mitchelmore, C.L., 2010. Accumulation and DNA damage in fathead minnows (*Pimephales promelas*) exposed to 2 brominated flame-retardant mixtures, Firemaster® 550 and Firemaster® BZ-54. *Environ Toxicol Chem* 29 (3), 722–729.
- [94] Sharma, P., Chadha, P., Saini, H.S., 2019. Tetrabromobisphenol A induced oxidative stress and genotoxicity in fish *Channa punctatus*. *Drug Chem Toxicol* 42 (6), 559–564.
- [95] Audebert, M., Dolo, L., Perdu, E., Cravedi, J.P., Zalko, D., 2011. Use of the  $\gamma$ H2AX assay for assessing the genotoxicity of bisphenol A and bisphenol F in human cell lines. *Arch Toxicol* 85 (11), 1463–1473.
- [96] Li, J., Moe, B., Vemula, S., Wang, W., Li, X.-F., 2016. Emerging disinfection byproducts, halobenzoquinones: effects of isomeric structure and halogen substitution on cytotoxicity, formation of reactive oxygen species, and genotoxicity. *Environ Sci Technol* 50 (13), 6744–6752.
- [97] Adhikari, A., Sen, M.M., Gupta-Bhattacharya, S., Chanda, S., 2004. Volumetric assessment of airborne fungi in two sections of a rural indoor dairy cattle shed. *Environ Int* 29 (8), 1071–1078.
- [98] Semple, R.K., Chatterjee, V.K., O’Rahilly, S., 2006. PPAR gamma and human metabolic disease. *J Clin Investig* 116 (3), 581–589.
- [99] Swedenborg, E., Rüegg, J., Mäkelä, S., Pongratz, I., 2009. Endocrine disruptive chemicals: mechanisms of action and involvement in metabolic disorders. *J Mol Endocrinol* 43 (1), 1–10.
- [100] Wang, Y., Zhang, W., Li, A., Song, M., 2021. Tetrachlorobisphenol A induced immunosuppression and uterine injury in mice. *Ecotoxicol Environ Saf* 207, 111527.